Determination of Formation Constants and Specific Ion Interaction Coefficients for $Ca_nUO_2(CO_3)_3^{(4-2n)-}$ Complexes in NaCl Solution by Time-Resolved Laser-Induced Luminescence Spectroscopy.

*Chengming Shang, Pascal E. Reiller**

[1] Den – Service d'Études Analytiques et de Réactivité des Surfaces (SEARS), CEA, Université Paris-Saclay, F-91191, Gif-sur-Yvette, France

*Corresponding author. Tel.: +33 1 6908 4312; fax: +33 1 6908 9475. E-mail address: pascal.reiller@cea.fr

http://doi.org/10.1039/C9DT03543E

Abstract

The formation constants of $CaUO_2(CO_3)_3^{2-}$ and $Ca_2UO_2(CO_3)_3(aq)$ were determined in NaCl medium at ionic strengths between 0.1 and 1 mol kg_w^{-1} using time-resolved laser-induced luminescence spectroscopy (TRLS). Spectroluminescence titration of $UO_2(CO_3)_3^{4-}$ complex by Ca^{2+} were conducted at atmospheric $CO_2(g)$ and varying pH values in order to eliminate the eventual precipitation of both schoepite ($UO_3{:}2H_2O$) and calcite ($CaCO_3$) in aqueous solutions. To identify the stoichiometry of calcium, the slope analyses corrected by the Ringböm coefficient for $UO_2(CO_3)_3^{4-}$ relative to pH and $CO_2(g)$ — instead of typical expression relative to UO_2^{2+} and CO_3^{2-} — was applied in this work. Satisfactory linear fits assessed the conditional stepwise formation constants in the range of ionic strength employed in this work, the values of which are in good agreement with literature data at comparable ionic strengths. Extrapolations to infinite dilution were realized in the framework of the specific ion interaction theory (SIT), also providing the evaluation of the specific ion interaction coefficients. The cumulative stability constants at infinite dilution was determined to be $\log_{10}\beta^\circ(CaUO_2(CO_3)_3^{2-}) = 27.20 \pm 0.04$ and $\log_{10}\beta^\circ(Ca_2UO_2(CO_3)_3(aq)) = 30.49 \pm 0.05$, which are in good agreement with extrapolation proposed elsewhere in literature using a different extrapolation framework. The specific ion interaction coefficients were found to be $\varepsilon(CaUO_2(CO_3)_3^{2-},Na^+) = (0.29 \pm 0.11)$ and $\varepsilon(Ca_2UO_2(CO_3)_3(aq),NaCl) = (0.66 \pm 0.12)$ kg_w mol^{-1}. Integration of alkali metals into the ternary species may explain these positive and relatively large interaction coefficients. Implications on the speciation of uranium in clay groundwaters, representative of radioactive waste repositories, and in seawater are discussed.

1. Introduction

The speciation of uranium is of great significance for a reliable prediction of its transport from disposal and storage sites of radioactive waste towards geosphere and biosphere. A variety of oxidation states and high coordination number complicates the chemical properties of uranium.[1,2] Hence, primary geochemical reactions — e.g., oxido-reduction, complexation with natural and anthropogenic ligands, and adsorption onto minerals — need to be carefully considered.[3] In particular, the ubiquitous presence of calcium and carbonate in natural water systems renders the formation and chemical behaviour of uranium in Ca-CO_3 rich waters important to be elucidated.[4] The $Ca_nUO_2(CO_3)_3^{(4-2n)-}$ complexes have been studied since their first identification in a seepage water from a uranium mine in Saxony, Germany.[5] Since then, several analytical methods were used to explore their chemical structures and behaviour, such as time-resolved laser-induced luminescence spectroscopy (TRLS),[5-11] anion exchange method,[12,13] potentiometry — using Ca-specific electrode —,[14] ultraviolet-visible (UV-Vis) absorption spectroscopy,[15] and extended X-ray absorption spectroscopy (EXAFS).[7,8,16-18] The interaction between Ca^{2+} and $UO_2(CO_3)_3^{4-}$ seems slightly more important compared to the other alkaline earth elements,.[12,13] but the typically more important concentration of calcium yield to a prevalence of $Ca_nUO_2(CO_3)_3^{(4-2n)}$ complexes over the other ternary species under environmental conditions in general, and potentially under envisaged disposal sites of nuclear waste in particular.[2,19] Adsorption experiments have showed that the formation of $Ca_nUO_2(CO_3)_3^{(4-2n)-}$ can influence U(VI) adsorption on minerals,[20,21] and enhance the mobility of uranium.[22,23] Therefore, the properties of $Ca_nUO_2(CO_3)_3^{(4-2n)-}$ complexes should be studied in detail, especially their thermodynamic binding constants, which are primordial for predictive modelling.

Among the methods mentioned above, TRLS is a highly sensitive technique to probe the characteristic features of luminescent species with limited disturbance of the aqueous equilibrium. The application to uranyl systems at low concentrations has proven the suitability and appropriateness in trace analysis of uranium.[24,25] The investigations of uranium(VI) hydrolysis have shown individual spectroscopic signatures of principle components after spectral decomposition of a series of experimental spectra as a function of pH.[26-28] However, uranyl complexation by carbonate has been considered faintly detectable by TRLS for a long time, which was attributable to the weak luminescence of UO_2-CO_3 at room temperature as a result of the quenching effects of carbonates.[29] More recently, authors have been able to collect the luminescence emission spectra of uranyl carbonate complexes and measure their decay-time,[6,30] even in a pronounced quenching environment like seawater.[17] The achievable acquisition of binary species spectrum permitted determining quantitatively the stability constants of ternary species with steadily enhanced luminescence intensity upon the association with alkaline earth cations.

Authors reported the stability constants of $Ca_nUO_2(CO_3)_3^{(4-2n)-}$ species in different electrolyte media based on similar thermodynamic considerations.[6,8,9,14] Titrations by calcium ion, generally at a fixed pH value, starting from a specific alkaline condition, where $UO_2(CO_3)_3^{4-}$ was dominating, to where the ternary species would take precedence. However, further investigations of experimental ranges suggest that aqueous conditions in literature may result in varying degrees of oversaturation with regard to calcite ($CaCO_3$) or schoepite ($UO_3{:}2H_2O$) in solution depending on the pH value — for calcite this was clearly shown by Dong and Brooks.[12] Endrizzi and Rao performed potentiometric titration at pH 10 in 0.1 mol L^{-1} NaCl using Ca^{2+} ion selective electrode.[14] The interfering effects of Na^+ and minor Mg^{2+} on the stability of electrode were confirmed to be absent in their work. Nevertheless, one can notice that another principal source of bias might emerge from the potential oversaturation of calcite at the reported pH value — even if this was clearly not observed. Similarly, in Kalmykov and Choppin,[9] onset of calcite precipitation might have occurred at pH 8.1 in 0.1 mol L^{-1} $NaClO_4$ because the end of spectroluminescent titration was conducted near the saturation limit of calcite. Moreover, Lee and Yun determined the formation constants at three pH values of 7.4, 8.1, and 9 in 0.1 mol L^{-1} $NaClO_4$.[6] Combined with an EDTA titration, it was found that $CaUO_2(CO_3)_3^{2-}$ was predominantly present at pH 8.1, and 9, and $Ca_2UO_2(CO_3)_3(aq)$ at pH 7.4 and higher Ca concentration. Their results could have also suffered from the same bias as the occurrence of schoepite (pH 7.4) and calcite (pH 8.1 and 9) were possible at different stages of titration.

Even though several thermodynamic constants have previously been reported, discrepancies in measured values and resulting theoretical calculations are worth mentioning. Up to now, none of these values have been selected in the critical review commissioned by the Thermochemical DataBase project of the Nuclear Energy Agency-Organization from the Economic Co-operation and Development (NEA-OECD, https://www.oecd-nea.org/dbtdb/)[31,32] — the implication of alkaline metal ions was suggested in Guillaumont, *et al.*[32] It should be noted that the relevant formation constants are must-have parameters for modelling the species distribution.[19]

The influence of background electrolyte effects on the ternary species received limited attention. Within the NEA-OECD selection of data, this particular aspect is dealt with using the specific interaction theory (SIT) — see Guillaumont, *et al.*[32] for details — through specific ion interaction coefficients ε between a complex and the oppositely charged ion from the background electrolyte. Equivocal implications of the reported ε values have been rarely assessed. To the best of our knowledge, only Dong and Brooks[13] proposed $\varepsilon(MgUO_2(CO_3)_3^{2-},Na^+) = -(3.0 \pm 0.3)$ kg_w mol^{-1} and re-evaluated $\varepsilon(Ca_2UO_2(CO_3)_3(aq),NaClO_4) = -2.7$ kg_w mol^{-1} from Kalmykov and Choppin.[9] Other authors postulated that $\varepsilon(MUO_2(CO_3)_3^{2-},Na^+)$ could be approximated in analogy to $\varepsilon(UO_2(CO_3)_2^{2-},Na^+)$

= -0.02 ± 0.09 $kg_w\ mol^{-1}$, and that $\varepsilon(Ca_2UO_2(CO_3)_3(aq),MX)$ was nil as commonly stated for non-charged species.[31,32] The very high ε values sometimes reported are reminiscent of theoretical calculation on the integration of alkaline ions into the structure of the $Ca_nUO_2(CO_3)_3^{(4-2n)-}$ complexes,[33] which remains to be demonstrated experimentally.

The scarcity of systematically determined specific ion interaction coefficients for this system is a major obstacle to the accurate speciation of uranium in natural media, and to specify whether the alkaline ions are capable of integrating into the manifold structures of ternary species at high ionic strengths.

To help answering these remaining questions, the aim of this work is to determine the thermodynamic formation constants of $Ca_nUO_2(CO_3)_3^{(4-2n)-}$ in NaCl using TRLS. The NaCl medium is chosen, instead of typical $NaClO_4$ for inert background electrolyte, for its relevance for natural waters, particularly for radioactive waste management sites.[34,35] It is also worthy to notice that these complex are of primordial importance in the context of uranium extraction from seawater.[14] The experiments are covering a large pH range excluding any possible precipitation of solid phases by modifying the total calcium concentration. The slope analyses of spectroluminescent titrations are used to identify the respective stability fields of the species and give information about their spectroscopic properties. The stepwise formation constants measured at various ionic strengths allow proposing the thermodynamic formation constants at infinite dilution, and the specific ion interaction coefficients $\varepsilon(CaUO_2(CO_3)_3^{2-},Na^+)$ and $\varepsilon(Ca_2UO_2(CO_3)_3(aq),NaCl)$, in the SIT framework. Practical application of the thermodynamic constants and specific ion interaction coefficients of the complexes will then be done for the estimation of uranium speciation in water compositions representative of radioactive waste management sites, and in seawater contexts as well.

2. Experimental Section

2.1. Materials

A stock solution of natural U(VI) was prepared after dissolution of U_3O_8 in 37 % hydrochloric acid (Sigma-Aldrich, ACS reagent) during one week. The aqueous concentration of uranium is measured by inductively coupled plasma mass spectroscopy (ICP-MS). The total uranium concentration in the experiments is maintained at 50 µmol kg_w^{-1} by diluting in NaCl solutions of different ionic strengths (0.1, 0.25, 0.5, 0.75 and 1 mol kg_w^{-1}), prepared with anhydrous NaCl (Sigma-Aldrich, ACS reagent, ≥ 99 %) and Millipore deionized water (Alpha-Q, 18.2 MΩ/cm). The observed spectral behaviour of U(VI), assumed to be the cumulative contribution of aqueous species, under saturated with respect to schoepite and calcite, is therefore an essential prerequisite for further acquisition. No precipitation effects has occurred at the present concentration of U(VI).

The pH values of the sample solutions were controlled in the range 7.4–9.0 with sodium hydroxide (Analytical Grade, Fisher) and diluted hydrochloric acid — the pH measurement protocol are detailed afterwards. The desired pH value is regularly checked and maintained unvaried in each analysed system throughout the experiments. The last measurement of pH value is done before TRLS analysis. Carbonate is introduced by adding appropriate amounts of freshly prepared $NaHCO_3$ solution (Analytical Grade, Fisher), calculated on the basis of equilibrium between aqueous solution and atmospheric CO_2(g). Calcium chloride (Sigma-Aldrich, ACS reagent, ≥ 99 %) is used to control the concentration of calcium. Sample solution is prepared in 15 mL polyethylene bottle and titrated with adequate amount of $CaCl_2$ solution. The volume of each required reagent is controlled as small as possible with the aim to maintain the ionic strength at the set value. All dilution are performed by weighing.

2.2. Determination of pH values and liquid junction potential

The measurements of pH values are performed at 22 °C. A combined-glass electrode (Mettler Toledo, USA) is calibrated routinely using four commercial solutions of pH 1.68, 4.01, 6.87 and 10.01 (SI Analytics, Mainz, Germany). A series of NaCl solutions of ionic strength from 0.1 to 3 mol kg_w^{-1} acidified by HCl to pcH (= $-\log_{10}[H^+]$) 2 was prepared to estimate the liquid junction potential.[36] The responses of potential read on the pH-meter against ionic strengths of NaCl solution were analysed in linear regression (not shown). The multi-point calibration method is applied in this study with aforementioned buffer solutions, the electrolyte concentrations of which are known.[37] The 95 % confidence limits are readily estimated by means of ordinary least squares,[38] which allowed the uncertainty of pH determination below 0.05 pH units.

For each measuring sample, the first pH adjustment is performed after introducing $NaHCO_3$ solution into the aqueous system. Then, the samples are let opened to the atmosphere during two hours. The values of pH would be slightly adjusted and checked for the second time, if there were any modifications. The final pH determination is carried out just before spectrum acquisition. The equilibrium with CO_2(g) can be confirmed by the fact that the pH values were almost unvarying after the additions of $NaHCO_3$(aq).

2.3. Time-Resolved Laser-Induced Luminescence Spectroscopy

A 2 mL solution of U(VI) is taken from the 15 mL polyethylene bottle and placed in a 1 cm quartz cuvette (QS101, Suprasil, Hellma Analytics). Prior to data acquisition, the cuvette is pre-equilibrated thermally at least 10 min in a controlled-temperature sample holder, connected to a thermostat (Peter Huber Kältemaschinenbau AG, Germany) with circulating water. A 355 nm tripled Nd:YAG laser (Surelite, Continiuum, USA) delivering about 170 mJ of energy is used as the laser excitation source, pulsed at 10 Hz with 5 ns pulse. An optical

parametric oscillator system (Horizon, Continiuum, USA) is set at λ_{ex} = 450 nm. The fluorescence cuvette is placed in a thermostated holder during measurements in order to minimize the temperature influence on uranyl luminescence.[39] The energy is monitored by a RJP-734 Joule-meter (Laser Probe, Inc.). The fluorescence signal is focused into a monochromator spectrometer (Acton) using a 300 lines mm^{-1} grating. An intensified CCD camera (Andor, UK) cooled by the Peltier effect (-10 °C) is used to detect the time-resolved fluorescence signal. Emission spectra are recorded as a function of gate delay D (≥ 25 ns, minimum for preventing the Raman scatter peak of H_2O) at the fixed gate width W = 1 µs. Following the expression of fluorescence signal in eq. 1, the collected spectra are then integrated over the same wavelength span to deduce the fluorescence intensity at various delay time. The concentration of U(VI) is low enough to eliminate the absorption effect of excitation and emission wavelength, *i.e.* the pre- and post-filter effects.

$$FI = \sum_i FI_0\ \tau_i \exp\left(-\frac{D}{\tau_i}\right)\left(1 - \exp\left(-\frac{W}{\tau_i}\right)\right) \quad (1)$$

where τ_i is fluorescence lifetime of species i, W is the gate width, FI represents fluorescence intensity at any given delay time and FI_0 is that at D = 0.

Spectral data management and analysis are carried out with Origin 9.0 software (OriginLab Corporation, USA) by a specially created data processing procedure. The Levenberg-Marquardt algorithm is used in least-square fitting method. The fluorescence intensities FI obtained at various delay time are fitted to an exponential decay function in order to derive the luminescence decay-time as well as the luminescence intensity at D = 0.[40-43] It is found that the decay time of Ca-UO_2-CO_3 species and delay time D are in the same order of magnitude. One prominent cause is that the luminescence intensity at D = 25 ns differed greatly from FI_0 and FI, thus should not be used in the analytical procedure for the sake of accuracy.

2.4. Correction for slope analysis

The methodological approach in this paper is based on the broader implications of previous studies.[5-15] As mentioned earlier, complexation of calcium with uranyl carbonate moiety has been investigated mainly by titration of calcium at fixed pH value. Such approaches, however, are restricted by the occurrence of schoepite and calcite. In spite of possible precipitation of minerals with actual concentrations of calcium(II) and uranium(VI), the speciation from literature improved our understanding of the Ca-UO_2-CO_3 system.

The predominance regions of calcium(II) and dicalcium(II) triscarbonatouranyl complexes are shown to evolve with pH and calcium concentration. More precisely, $CaUO_2(CO_3)_3^{2-}$ occurs at relatively high pH and low calcium concentration, while lower pH and higher calcium concentration favours $Ca_2UO_2(CO_3)_3(aq)$. For ruling out the undesired precipitations, a titration of calcium at varying pH values is used in this study. The degree of complexation is estimated by the variation of fluorescence intensity as a function of the free Ca^{2+} concentration. By these means, the stoichiometry of ternary species is identified by the so-called slope analysis, which provided an approach to investigate separately their properties. Preliminary calculations are performed with literature data.[12] It appears that simultaneously changed pH values and Ca^{2+} concentrations allow the successive complexation to such an extent that the fractions of $CaUO_2(CO_3)_3^{2-}$ and $Ca_2UO_2(CO_3)_3(aq)$ could attain up to 50-85 % in the middle and at the end of entire titration, respectively — see Figure S1, and the aqueous conditions are listed in Table S1 of the Supplementary Information (SI). Stepwise formations of $CaUO_2(CO_3)_3^{2-}$ and $Ca_2UO_2(CO_3)_3(aq)$ are described with the stepwise equilibrium constants $K_{n.1.3}$ at a given ionic strength expressed as follows,

$$nCa^{2+} + UO_2(CO_3)_3^{4-} \rightleftarrows Ca_nUO_2(CO_3)_3^{(4-2n)-}$$

$$K_{n,1,3} = \frac{\left[Ca_nUO_2(CO_3)_3^{(4-2n)-}\right]}{\left[Ca^{2+}\right]^n \left[UO_2(CO_3)_3^{4-}\right]} \quad (2)$$

where squared brackets indicate concentration on molality scale (mol kg_w^{-1}).

As represented in eq. 4, the slope n stands for the stoichiometric number of calcium ion involved, R is the concentration ratio between complexed and non-complexed uranyl carbonate moiety by calcium considering the influence of pH, and the intercepts $\log_{10}K_{n.1.3}$ refer to the stepwise formation constants of $Ca_nUO_2(CO_3)_3^{(4-2n)-}$ and $Ca_2UO_2(CO_3)_3(aq)$ at a particular ionic strength value.

$$\log_{10}R = \log_{10}\frac{\left[Ca_nUO_2(CO_3)_3^{(4-2n)-}\right]}{\left[UO_2(CO_3)_3^{4-}\right]/\alpha} = \log_{10}K_{n,1,3} + n\log_{10}[Ca^{2+}] \quad (3)$$

This latter expression can be expressed as luminescence intensity,

$$\log_{10}R = \log_{10}\frac{FI_0\left(Ca_nUO_2(CO_3)_3^{(4-2n)-}\right)}{FI_0\left(UO_2(CO_3)_3^{4-}\right)/\alpha} = \log_{10}K_{n.1.3} + n\log_{10}[Ca^{2+}] \quad (4)$$

where $FI_0(Ca_nUO_2(CO_3)_3^{(4-2n)-})$ is the fluorescence intensity extrapolated at $D = 0$ of the complexed species at variable pH values, $FI_0(UO_2(CO_3)_3^{4-})$ is that of the non-complexed triscarbonatouranyl moiety at pH 9, and α represents the Ringböm[44] coefficient of $UO_2(CO_3)_3^{4-}$. It is calculated to assess the variation of aqueous content of triscarbonatouranyl with pH (vide infra), since the denominator of R refers to the amount of $UO_2(CO_3)_3^{4-}$ at the same pH value with the numerator sample but at $[Ca^{2+}] = 0$ conditions.

2.5. Calculation of the Ringböm coefficient relative to $UO_2(CO_3)_3^{4-}$

The investigated pH range varied from a circum neutral condition about pH 7.4 to a mildly alkaline condition at pH ca. 9.0. The highest pH value leads to the predominance of $UO_2(CO_3)_3^{4-}$ in atmospherically-equilibrated aqueous solution, owing to the dissolution of $CO_2(g)$ in $H_2CO_3(aq)$, HCO_3^-, and CO_3^{2-}. In contrast, in neutral to mildly alkaline conditions without calcium, complicated speciation of uranium(VI) driven by hydrolysis and oligomerization, even possible precipitation of $UO_3{:}2H_2O(cr)$, would render the prediction of individual concentration for all the involved species difficult. For this reason, direct fluorescence measurement of uranyl-carbonate solutions prepared at investigated pH values without calcium is untenable, as characteristic fluorescence properties would be inevitably interfered by hydroxo uranyl species. Fluorescence decay spectra of a sample prepared at pH 7.6 were acquired over a large range of delay time, where the spectral profiles were significantly affected as shown in Figure S2 of the SI.

Many previous studies of uranyl carbonate system showed that when the solution suffered a decrease in pH, starting from a highly alkaline condition, the proportion of $UO_2(CO_3)_3^{4-}$ crucially decreased as the less-complexed species — e.g., $UO_2(CO_3)_2^{2-}$, $UO_2CO_3(aq)$ —, the hydroxo species — e.g., $UO_2(OH)^+$, $UO_2(OH)_2(aq)$ — and the polynuclear species — e.g., $(UO_2)_2CO_3(OH)_3^-$, $(UO_2)_3(OH)_5^+$… — increased.[28,29,45-47] To reconcile these aqueous features of hydroxo and carbonato uranyl complexes, we postulated that $UO_2(CO_3)_3^{4-}$ contributed primarily to the variation of non-complexed by calcium species as a function of pH, over other hydroxides and carbonates species in calcium-uranium(VI)-carbonate system. Consequently, evaluation of the Ringböm[44] coefficient α at different pH values in free-calcium conditions sufficed to estimate the impact of pH values. The assumption is then validated by speciation calculation with determined thermodynamic data in this work.

The typical description and thermodynamic formation constant of hydrolysis-carbonation equilibria are often written relative to uranyl(VI) species UO_2^{2+} and CO_3^{2-} as follows.

$$m\mathrm{UO_2^{2+}} + n\mathrm{H_2O} + q\mathrm{CO_3^{2-}} \rightleftarrows (\mathrm{UO_2})_m(\mathrm{CO_3})_q(\mathrm{OH})_n^{(2m-n-2q)+} + n\mathrm{H^+}$$

$$\log_{10}\beta^\circ_{m.n.q} = \frac{\left[(\mathrm{UO_2})_m(\mathrm{CO_3})_q(\mathrm{OH})_n^{(2m-n-2q)+}\right]\left[\mathrm{H^+}\right]^n}{\left[\mathrm{UO_2^{2+}}\right]^m\left[\mathrm{CO_3^{2-}}\right]^q} \quad (5)$$

Varying pH values means that CO_3^{2-} concentrations should be recalculated. In our case, it seems more convenient to express the complexation relative to $UO_2(CO_3)_3^{4-}$ and partial pressure of CO_2(g) as follows instead.

$$m\mathrm{UO_2(CO_3)_3^{4-}} + (6m-2q-n)\mathrm{H^+} \rightleftarrows (\mathrm{UO_2})_m(\mathrm{CO_3})_q(\mathrm{OH})_n^{(2m-n-2q)+} + (3m-q)\mathrm{CO_2(g)} + (3m-q-n)\mathrm{H_2O}$$

$$\log_{10}\beta'^\circ_{m.n.q} = \frac{\left[(\mathrm{UO_2})_m(\mathrm{CO_3})_q(\mathrm{OH})_n^{(2m-n-2q)+}\right]P(\mathrm{CO_2})^{(3m-q)}}{\left[\mathrm{UO_2(CO_3)_3^{4-}}\right]^m\left[\mathrm{H^+}\right]^{(6m-2q-n)}} \quad (6)$$

The thermodynamic constant can be calculated from the selected thermodynamic data from Guillaumont et al.[32] as follows,

$$\log_{10}\beta'^\circ_{m.n.q} = \log_{10}\beta^\circ_{m.n.q} - \mathrm{m}\log_{10}\beta^\circ_{1.0.3} - (3m-q)\log_{10}\beta^\circ_{0.1.1} \quad (7)$$

or directly form the Gibbs energy of formation, $\Delta_f G^\circ_m$.

The concentration of $UO_2(CO_3)_3^{4-}$ at each pH value can then be expressed only as a function of $[H^+]$ and $P(CO_2)$ using the constants calculated from the known $\Delta_f G^\circ_m$ taken from the NEA-OECD database,[32] as listed in Table 1 and Table 2, using the mass action law.

The Ringböm coefficient is introduced to quantify the fraction of U(VI) present as the $UO_2(CO_3)_3^{4-}$ complex with the mass balance on $UO_2(CO_3)_3^{4-}$ expressed in eq. (8). The mathematical form is slightly simplified to a quadratic equation with one unknown as $UO_2(CO_3)_3^{4-}$ by neglecting lesser contributing terms from hydrolysed species $(UO_2)_n(OH)_m^{(2n-m)+}$.

$$C_T = \left[\mathrm{UO_2(CO_3)_3^{4-}}\right] + \left(1 + \beta'_{1.0.2}\frac{\left[\mathrm{H^+}\right]}{P(\mathrm{CO_2})} + \beta'_{1.0.1}\frac{\left[\mathrm{H^+}\right]^4}{P(\mathrm{CO_2})^2}\right) + 2\beta'_{2.3.1}\frac{\left[\mathrm{UO_2(CO_3)_3^{4-}}\right]^2\left[\mathrm{H^+}\right]^7}{\mathrm{P(CO_2)^5}} \quad (8)$$

where α = $C_T/[UO_2(CO_3)_3^{4-}]$, $P(CO_2) = 10^{-3.5}$ atm, and $[H^+]$ is converted from (H^+), measured by pH-meter. The calculation of $\beta'_{m.n.l}$ required a correction of the water activity a_{H_2O} for each ionic strength — see eq. B.9 from Guillaumont, *et al.*[32] Ringböm coefficient was calculated for each sample at specified values of pH and ionic strength (Table S2 of the SI).

Table 1. Stability constants of U(VI) complexes at 25 °C and I_m = 0, used in the work.

Reaction	$\log_{10} K^\circ$	References
$CO_2(g) + H_2O \rightleftarrows CO_3^{2-} + 2H^+$	-18.15 ± 0.06	[32]
$UO_2^{2+} + H_2O \rightleftarrows UO_2(OH)^+ + H^+$	-5.25 ± 0.24	[32]
$UO_2^{2+} + 2H_2O \rightleftarrows UO_2(OH)_2(aq) + 2H^+$	-12.15 ± 0.07	[32]
$3\ UO_2^{2+} + 5H_2O \rightleftarrows (UO_2)_3(OH)_5^+ + 5H^+$	-15.55 ± 0.12	[32]
$UO_2^{2+} + CO_3^{2-} \rightleftarrows UO_2(CO_3)(aq)$	9.94 ± 0.03	[32]
$UO_2^{2+} + 2\ CO_3^{2-} \rightleftarrows UO_2(CO_3)_2^{2-}$	16.61 ± 0.09	[32]
$UO_2^{2+} + 3\ CO_3^{2-} \rightleftarrows UO_2(CO_3)_3^{4-}$	21.84 ± 0.04	[32]
$2\ UO_2^{2+} + CO_2(g) + 4H_2O \rightleftarrows (UO_2)_2CO_3(OH)_3^- + 5H^+$	-19.01 ± 0.50	[32]
$UO_2(CO_3)_3^{4-} + 4H^+ \rightleftarrows UO_2(CO_3)(aq) + 2CO_2(g) + 2H_2O$	24.40 ± 0.21*	Recalculated from[32]
$UO_2(CO_3)_3^{4-} + 2H^+ \rightleftarrows UO_2(CO_3)_2^{2-} + CO_2(g) + H_2O$	12.92 ± 0.15*	Recalculated from[32]
$2\ UO_2(CO_3)_3^{4-} + 7\ H^+ \rightleftarrows (UO_2)_2CO_3(OH)_3^- + 5CO_2(g) + 2H_2O$	46.21 ± 0.70*	Recalculated from[32]
$Ca^{2+} + UO_2(CO_3)_3^{4-} \rightleftarrows CaUO_2(CO_3)_3^{2-}$	5.26 ± 0.01	This work
$2Ca^{2+} + UO_2(CO_3)_3^{4-} \rightleftarrows Ca_2UO_2(CO_3)_3(aq)$	8.65 ± 0.02	This work
$Ca^{2+} + UO_2^{2+} + 3\ CO_3^{2-} \rightleftarrows CaUO_2(CO_3)_3^{2-}$	27.20 ± 0.04	This work
$2Ca^{2+} + UO_2^{2+} + 3\ CO_3^{2-} \rightleftarrows Ca_2UO_2(CO_3)_3(aq)$	30.49 ± 0.05	This work

Table 2. Gibbs energies of formation from the main species considered within this work.

Species	$\Delta_f G°_m$ (kJ mol^{-1})	References
H_2O	-237.140 ± 0.041	[32]
$CO_2(g)$	-394.373 ± 0.133	[32]
CO_3^{2-}	-527.900 ± 0.390	[32]
UO_2^{2+}	-952.551 ±1.747	[32]
$UO_2(CO_3)_3^{4-}$	-2 660.914 ± 2.116	[32]
$(UO_2)_2CO_3(OH)_3^-$	-3 139.526 ± 4.517	[32]
Ca^{2+}	-552.806 ± 1.050	[32]
$CaUO_2(CO_3)_3^{2-}$	-3 244.316 ± 2.361	This work
$Ca_2UO_2(CO_3)_3(aq)$	-3 815.901 ± 2.985	This work

2.6. Specific ion interaction theory (SIT)

The SIT approach,[32] used to extrapolate the thermodynamic constants to infinite dilution, is applicable to a wider range of ionic strength compared to the Davies equation.[48] Thus, the SIT is employed to extrapolate the conditional formation constants to infinite dilution condition, and determine the specific ion interaction coefficients $\varepsilon(CaUO_2(CO_3)_3^{2-},Na^+)$ and $\varepsilon(Ca_2UO_2(CO_3)_3(aq),NaCl)$. The activity coefficient is expressed as follows,

$$\log_{10}\gamma = - z_j^2 D_H + \varepsilon(j,k,I_m)\, m_k \quad (9)$$

with D_H the Debye-Hückel term,

$$D_H = \frac{A\sqrt{I_m}}{1 + 1.5\sqrt{I_m}} \quad (10)$$

where I_m is the ionic strength on the molal scale, ε represents the ion interaction coefficient (kg_w mol^{-1}) and m_k is the concentration of background electrolyte k in molality.

The value of 0.507 kg$^{1/2}$ mol$^{-1/2}$ is assigned to A at 22 °C.[32] The correlation between stepwise formation constants and ionic strengths can be drawn by the following relationship:

$$\log_{10}K_{n.1.3} = \log_{10}K°_{n.1.3} + \Delta z^2 D_H - \Delta\varepsilon\, I_m \quad (11)$$

where

$$\Delta z^2 = z\left(Ca_nUO_2(CO_3)_3^{(4-2n)-}\right)^2 - n\, z(Ca^{2+})^2 - z\left(UO_2(CO_3)_3^{4-}\right)^2 \qquad (12)$$

($\Delta z^2 = -16$ for n = 1 and $\Delta z^2 = -24$ for n = 2)

and

$$\Delta\varepsilon = \varepsilon(Ca_nUO_2(CO_3)_3^{(4-2n)-},Na^+) - n\,\varepsilon(Ca^{2+},Cl^-) - \varepsilon(UO_2(CO_3)_3^{4-},Na^+) \qquad (13)$$

The main specific ion interaction coefficients used in this work are reported in Table 3.

Table 3. Main specific ion interaction coefficients used in this work.

Specific ion interaction coefficient	Value (± 1σ)	Reference
$\varepsilon(H^+,Cl^-)$	0.12 ± 0.01	[32]
$\varepsilon(Na^+,CO_3^{2-})$	-0.08 ± 0.03	[32]
$\varepsilon(UO_2^{2+},Cl^-)$	0.21 ± 0.02	[32]
$\varepsilon(Ca^{2+},Cl^-)$	0.14 ± 0.01	[32]
$\varepsilon(UO_2(CO_3)_2^{2-},Na^+)$	-0.02 ± 0.09	[32]
$\varepsilon(UO_2(CO_3)_3^{4-},Na^+)$	-0.01 ± 0.11	[32]
$\varepsilon(CaUO_2(CO_3)_3^{2-},Na^+)$	0.29 ± 0.11	This work
$\varepsilon(Ca_2UO_2(CO_3)_3(aq),NaCl)$	0.66 ± 0.12	This work

3. Results and discussion

3.1. Evolution of luminescence spectra

The upper limit of aqueous electrolyte concentration is imposed to 1 mol kg_w^{-1} NaCl considering the noticeable quenching effect of chloride ions.[49] Five series of solutions are separately prepared at designed ionic strengths. The fluorescence spectra of aqueous Ca-UO_2-CO_3 complexes at I_m = 0.5 mol kg_w^{-1} NaCl are shown in Figure 1 — those of the four other series are shown in Figure S3 of the SI. A total of 100 sample fluorescence spectra acquired at D = 25 ns were imported into Origin 9.0 software for Gaussian-based peak separation analysis. Characteristic peak wavelengths found at 464.31 ± 0.38, 483.30 ± 0.30, 503.18 ± 0.29, 524.26 ± 0.76 and 546.96 ± 2.25 nm (weighed average of all peak maxima with 2σ uncertainties) are in agreement with literature values.[6,8,9] Hypsochromic-shifted peak positions compared with those of uranyl ions (470.07, 487.31, 509.31, 533.38 and 559.86 nm) in acidic conditions provide evidence for the inner-sphere substitution of carbonate groups for water molecules (Figure S4 of the SI).[50] Fluorescence spectral profiles and band positions do not show any change irrespective of varying aqueous conditions, i.e.

Ca^{2+} concentration and pH value. This observation indicates that energy transfer between excited electronic state and distinct vibrational levels of ground electronic state is less susceptible to the binding of additional Ca^{2+} ions.

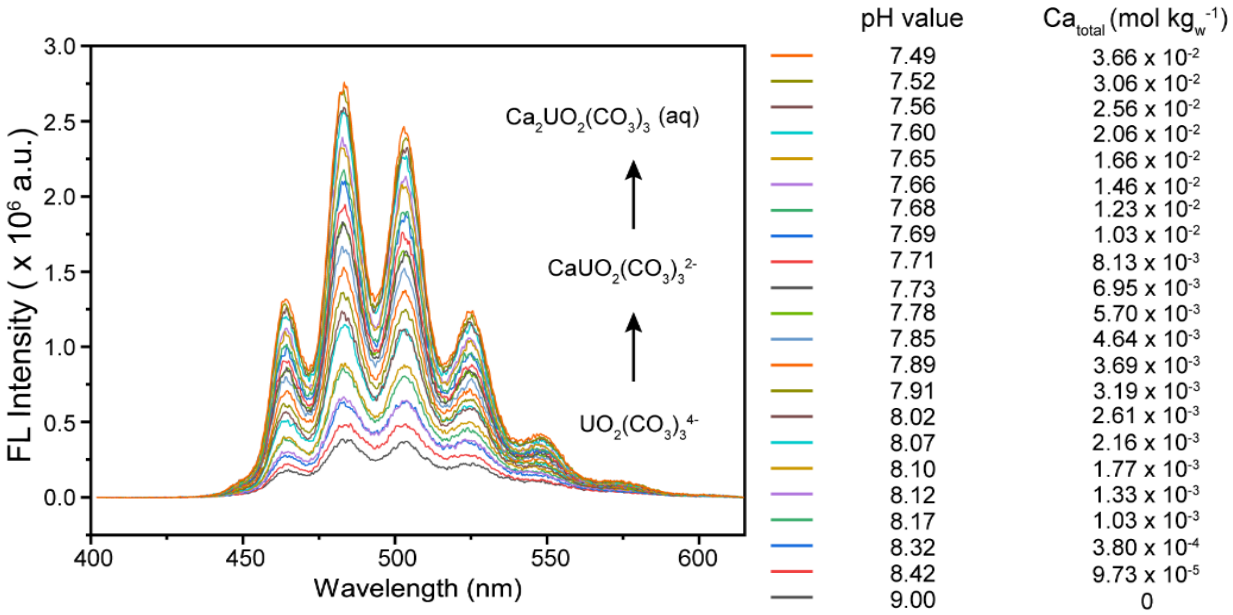


Figure 1. Measured luminescence emission spectra of uranium(VI) at various calcium concentrations and pH values, $P(CO_2) = 10^{-3.5}$ *atm, and* $I_m = 0.5$ *mol* kg_w^{-1} *NaCl; initial delay time of* D *= 25 ns and gate width* W *= 1 μs, number of accumulation is 1000.*

Successive complexation reactions of calcium ions with triscarbonatouranyl moiety give information about the characters of the studied complexes, resulting from gradually enhanced fluorescence intensity, better-resolved spectrum, and slower luminescence decay-time. Similar trend of spectral and temporal features are observed for every measuring series. The continuously increasing luminescence intensity and decay-time illustrate the progressive complexation of calcium ions. The observed tendency is in line with the sequentially conformational change from $CaUO_2(CO_3)_3^{2-}$ to $Ca_2UO_2(CO_3)_3(aq)$ in aqueous solution.

Luminescence decay-times are determined by fitting the integrated time-resolved luminescence intensities to exponential decay functions. The slope analysis results are used to clarify the borderlines of predominant regions of $CaUO_2(CO_3)_3^{2-}$ and $Ca_2UO_2(CO_3)_3(aq)$ complexes.

Graphical representation of $\log_{10}R$ vs. $\log_{10}[Ca^{2+}]$ allows a straightforward examination of complexation. The aqueous calcium ion is assumed to be present as free Ca^{2+}, since the analytical concentration of calcium is at least 10 times as large as that of U(VI). This simplification is attended by the fact that the amount of calcium consumed in the complexation is negligible with regard to its initial concentration.[51] The experimental data are fitted to straight lines using a least square method,[52] the slopes representing the stoichiometry of Ca^{2+} ions bound to triscarbonatouranyl complex, the intercepts are assigned to the stepwise equilibrium constants at specific background electrolyte concentration. Linear relationships between $\log_{10}R$ and $\log_{10}[Ca^{2+}]$ are obtained with slopes changing from ca. 1 to ca. 2 as Ca^{2+} is added into the solution (Figure 2). This also demonstrates conclusive evidence for successive formations of $CaUO_2(CO_3)_3^{2-}$ then $Ca_2UO_2(CO_3)_3(aq)$.

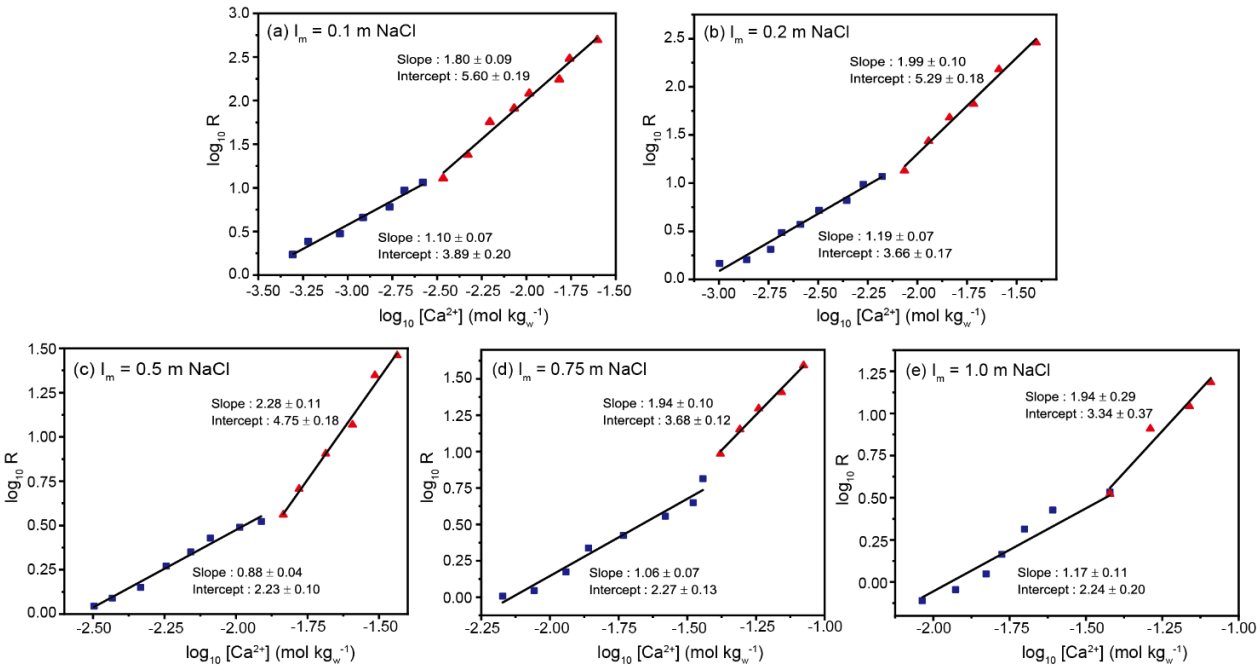


Figure 2. Logarithmic ratio R in terms of luminescence intensity and Ringböm coefficient plotted as a function of $log_{10}[Ca^{2+}]$ (mol kg_w^{-1}) at investigated NaCl ionic strengths: $[U]_{total}$ = 50 µmol kg_w^{-1}, P$(CO_2) = 10^{-3.5}$ atm.

The respective decay-times are deduced by averaging the measured decay-times of correspondent sample solutions. It is assessed that in 0.1 mol kg_w^{-1} NaCl medium, $UO_2(CO_3)_3^{4-}$ is showing a fast decay-time of $\tau(UO_2(CO_3)_3^{4-})$ =(11.04 ± 0.11) ns, compared with $\tau(CaUO_2(CO_3)_3^{2-})$ = (28.30 ± 0.57) ns and $\tau(Ca_2UO_2(CO_3)_3(aq))$ = (46.7 ± 2.7) ns. The possible quenching effect of chloride on luminescence decay-time make it moderately meaningful to compare our results with those in literature, generally in non-complexing medium (0.1 mol L^-

[1] Na/$HClO_4$),[6,8] albeit measured decay-times are numerically comparable with each other. In addition, a noticeable suppression of Ca-UO_2-CO_3 complexes decay-times is observed at larger NaCl concentrations that gives a clue to information such as quenching rate constant, which would require deeper attention in further works.

Only mono-exponential functions are needed to fit the intensity decay curves, though at least two calcium triscarbonatouranyl complexes are expected to exist in the majority of the samples. Two representative exponential fits at ionic strength of 0.1 mol kg_w^{-1} NaCl are shown in Figure 3. Single exponential decay generally suggests that either only one luminescent species is observed, or the rate of de-excitation process is faster than that of ligand exchange. Nevertheless, for such a complex system containing rather complicated fluorophores, luminescence decay behaviour cannot be simply settled. Our observations are in accordance with previous studies as the same decay mode has been observed otherwise for Ca-UO_2-CO_3 ternary system.[6,8] However, a recent study showed clear multi-exponential decays in Mg-UO_2-CO_3 system, from which the characteristic decay times for principle U(VI) species were determined.[7]

Numerous mutually exclusive mechanisms, especially in photochemistry, have been proposed to interpret the inconsistencies in decay mode between Ca/Mg-UO_2-CO_3 systems, e.g., hydrogen abstraction,[53] formation of exciplex,[54] and reversible intersystem crossing.[55] Unfortunately, these mechanisms are not likely to explain the discrepancy between experimental results, as the complexation of Ca/Mg is likely to occur outside the first coordination sphere. It seems more likely that the shorter distance of U-Mg (3.84 Å) compared to that of U-Ca (4.15 Å) could reason out the difference in fluorescent properties.[7]

Several emission spectra of different compositions in binary/ternary species at I_m = 0.2 and 1 mol kg_w^{-1} are normalized to their total area in order to compare the spectroscopic changes (Figure 4). The percentage of species are calculated with the determined formation constants (vide post) for $CaUO_2(CO_3)_3^{2-}$ and $Ca_2UO_2(CO_3)_3$(aq). Unambiguously, the increase in Ca^{2+} concentration makes no distinctive difference in peak positions, but results in clearly better resolved spectra and narrow peak widths. The similar spectral trends have been observed elsewhere.[6,7] It must be noted that the use of the 300 lines mm^{-1} grid favours convolution of the different components with the parameters of the optical set-up. The use of a grid with a higher resolution could help in the deconvolution of the signal and identifying spectral differences.[56]

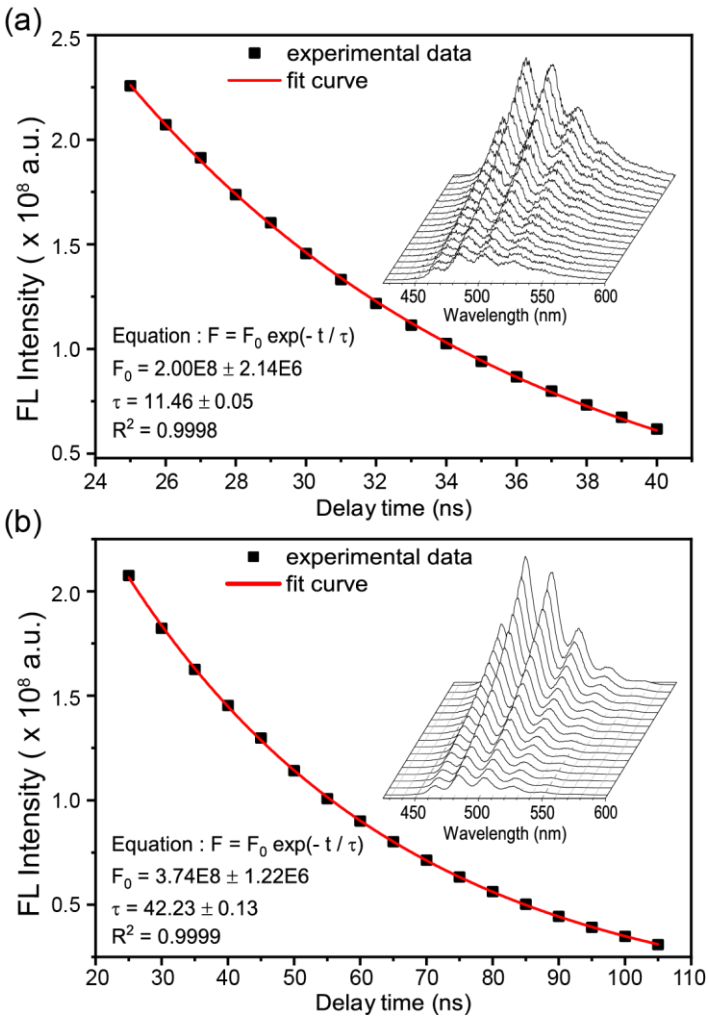


Figure 3. Mono-exponential fits of luminescence intensity decay of (a) $UO_2(CO_3)_3^{4-}$ at [U(VI)] = 50 µmol kg_w^{-1} and pH = 9.0, and (b) Ca-UO_2-CO_3 complexes at [U(VI)] = 50 µmol kg_w^{-1}, $log_{10}[Ca^{2+}]$ = -2.06, pH = 7.60 and I_m = 0.1 mol kg_w^{-1} NaCl. The insets show the waterfall plots of luminescence emission spectra as a function of delay time.

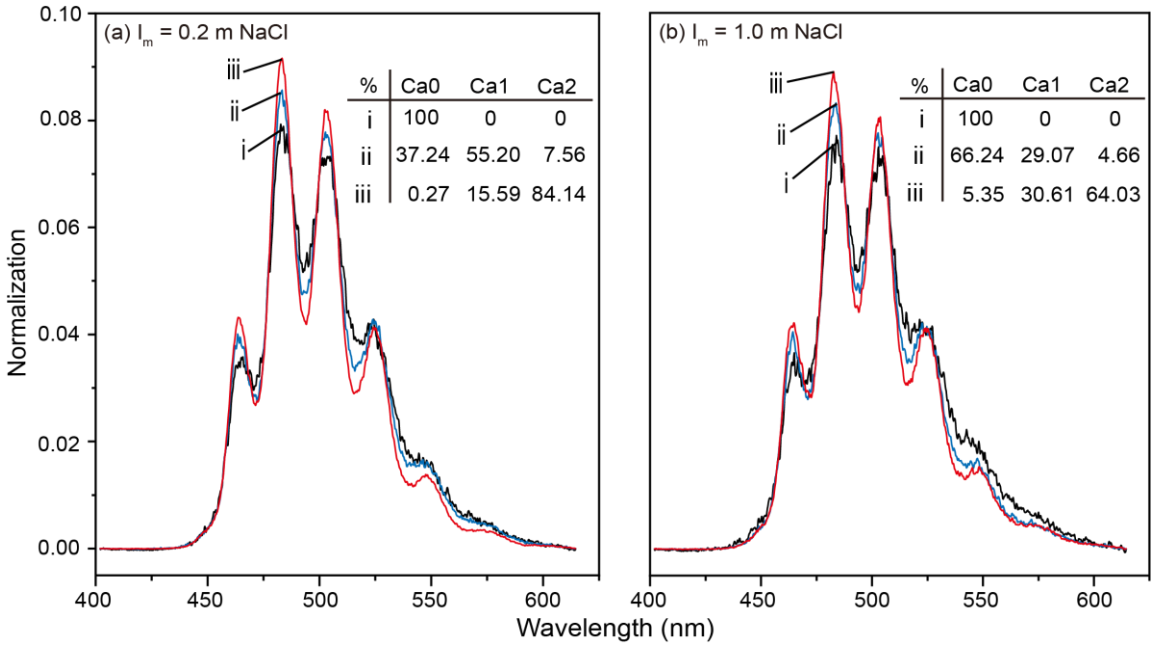


Figure 4. Luminescence emission spectra normalized to the same area at D *= 25 ns of (Ca-)UO_2-CO_3 species at (a) I_m = 0.2 mol kg_w^{-1}, and (b) 1 mol kg_w^{-1}; Ca0, Ca1, and Ca2 stand for $UO_2(CO_3)_3^{4-}$, $CaUO_2(CO_3)_3^{2-}$, and $Ca_2UO_2(CO_3)_3(aq)$, respectively.*

3.2. Evaluation of equilibrium constants and specific ion interaction coefficients

The graphical results in previous section provide insights into the fluorescence behaviour and complexation mechanism of the investigated system. The quenching effect of chloride is susceptible to affect the applicability of slope analysis method at high concentration, *ca.* 1 mol kg_w^{-1} NaCl, given that the experimental points at $\log_{10}([Ca^{2+}]$ mol $kg_w^{-1})$ ≥ -1.1 deviates from the linear trend — not shown in **Figure 2**. A possible explanation is probably associated with some artefacts altering the measurements of emission spectra. Because of the concentrated electrolyte, the system required a raising quantity of calcium to overcome the electrostatic force for the formation of the ternary species. This fact led to a significant increase in the actual ionic strength as a result of the contribution of $[Ca^{2+}]$, which in turn made the impact of polarization and viscosity on fluorescence too important to be neglected.[57] However, it is yet unclear to which extent the spectral features are influenced. Notwithstanding the sparse experimental points, acceptable linear fits were retained at I_m = 1 mol kg_w^{-1}.

The calcium concentrations for predominance regions of the $Ca_nUO_2(CO_3)_3^{(4-2n)-}$ species can be read directly from Figure 4. Table 4 summarizes the detailed solution information of

calcium concentrations and pH values for every species being predominantly present. Converting back from the logarithmic form, one can infer that the predominance range of $CaUO_2(CO_3)_3^{2-}$ enlarges with ionic strength, as a result of increasing interionic attraction between Ca^{2+} and Cl^-.

Table 4. Values of decimal logarithm of calcium concentration (mol kg_w^{-1}) extracted from the slope analysis in Figure 4, and pH values measured before luminescence acquisition.

I_m (mol kg_w^{-1})	$CaUO_2(CO_3)_3^{2-}$	$Ca_2UO_2(CO_3)_3(aq)$
0.10	$-3.35 \le \log_{10}[Ca^{2+}] \le -2.58$	$-2.58 \le \log_{10}[Ca^{2+}] \le -1.52$
	$8.10 \le pH \le 7.85$	$7.85 \le pH \le 7.45$
0.20	$-3.00 \le \log_{10}[Ca^{2+}] \le -2.15$	$-2.15 \le \log_{10}[Ca^{2+}] \le -1.41$
	$8.14 \le pH \le 7.75$	$7.75 \le pH \le 7.40$
0.50	$-2.50 \le \log_{10}[Ca^{2+}] \le -1.87$	$-1.87 \le \log_{10}[Ca^{2+}] \le -1.43$
	$7.91 \le pH \le 7.68$	$7.68 \le pH \le 7.49$
0.75	$-2.20 \le \log_{10}[Ca^{2+}] \le -1.44$	$-1.44 \le \log_{10}[Ca^{2+}] \le -1.07$
	$7.79 \le pH \le 7.52$	$7.52 \le pH \le 7.39$
1.00	$-2.12 \le \log_{10}[Ca^{2+}] \le -1.40$	$-1.40 \le \log_{10}[Ca^{2+}] \le -1.08$
	$7.86 \le pH \le 7.54$	$7.54 \le pH \le 7.40$

The binding constants of Ca^{2+} ion to $CaUO_2(CO_3)_3^{2-}$, noted as $\Delta\log_{10}K$, are 2.43, 2.13, 1.79, 1.59, and 1.51 by subtracting $\log_{10}K_{1.1.3}$ from $\log_{10}K_{2.1.3}$. It is found that $\Delta\log_{10}K$ is lower than $\log_{10}K_{1.1.3}$ at each ionic strength, revealing that the binding of Ca^{2+} to $CaUO_2(CO_3)_3^{2-}$ is more difficult than that of Ca^{2+} to $UO_2(CO_3)_3^{4-}$. This is expected because the electrostatic interaction is stronger between $Ca^{2+}/UO_2(CO_3)_3^{4-}$ than that between $Ca^{2+}/CaUO_2(CO_3)_3^{2-}$ due to the stepwise charge neutralization.

The resulting conditional equilibrium constants after rounding off the slope values to their nearest integers are given in Table S3 of the SI. By comparing the different ionic strength series, one can immediately assess the tendency of the stability of ternary species. The dependence of $\log_{10}K_{1.1.3} + 16D$ and $\log_{10}K_{2.1.3} + 24D$ vs. the molal ionic strength in NaCl is represented in Figure 5. The two plots both give a linear relationships over the entire range of ionic strength, which allow determining the ion interaction coefficients and the stepwise formation constants by extrapolating to infinite dilution using the SIT to $\log_{10}K^\circ_{1.1.3} = 5.36 \pm 0.02$ and $\log_{10}K^\circ_{2.1.3} = 8.65 \pm 0.02$. For $CaUO_2(CO_3)_3^{2-}$ and $Ca_2UO_2(CO_3)_3(aq)$, the cumulative formation constants are $\log_{10}\beta^\circ_{1.1.3} = 27.20 \pm 0.04$ and $\log_{10}\beta^\circ_{2.1.3} = 30.49 \pm 0.05$, respectively — see Table 1, and see $\Delta_f G^\circ_m$ in Table 2. The ion interaction coefficients are

evaluated to be $\varepsilon(CaUO_2(CO_3)_3^{2-},Na^+)$ = (0.29 ± 0.11) and $\varepsilon(Ca_2UO_2(CO_3)_3(aq),NaCl)$ = (0.66 ± 0.12) $kg_w\ mol^{-1}$. The mean values and respective uncertainties for $\log_{10}\beta^\circ$ and ε are estimated using the weighed linear regression with reciprocals of the squared standard deviation ($1/\sigma_i^2$) as weights,[58] determined from the slope analysis. The uncertainty range is assessed by propagating the uncertainties from I_m = 0 up to 1 mol kg_w^{-1}. The successive calcium complexes display increasing overall formation constants, which mirrors the stability of the ternary complexes. The obtained values for $\log_{10}\beta^\circ_{1.1.3}$ and $\log_{10}\beta^\circ_{2.1.3}$ are consistent with literature data[12,14] within the uncertainty limits.

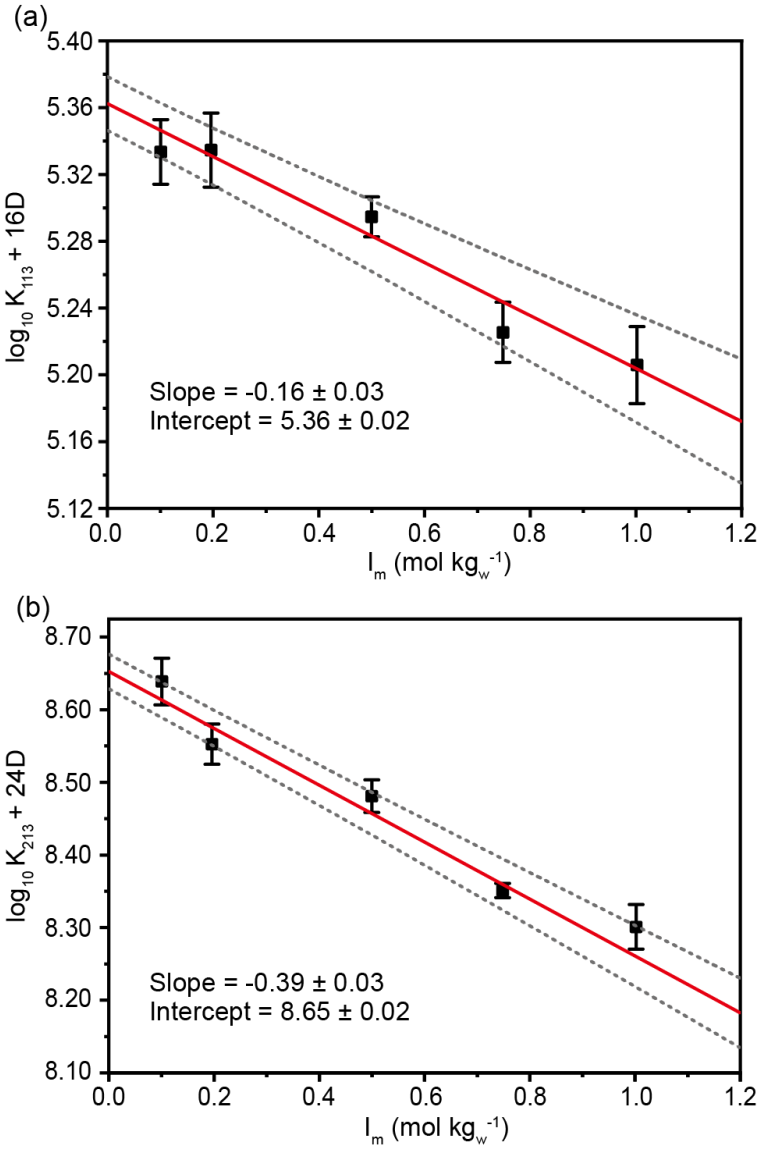


Figure 5. Extrapolation to infinite dilution of the experimental data of (a) $\log_{10}K_{1.1.3}$ + 16D and (b) $\log_{10}K_{2.1.3}$ + 24D as a function of molal ionic strength.

The predominance diagram at I_m = 0.2 mol kg_w^{-1} NaCl in Figure 6 is constructed from our newly determined $\log_{10}\beta^{\circ}_{n.1.3}$ and ε values using PhreePlot,[59,60] which includes PhreeqC[61,62] that handles the SIT. The apparent precipitation region of calcite, limited by the black dashed line, is imposed by the equilibrium between the atmospheric CO_2(g) and the aqueous solution — the four other series are shown in Figure S5 of the SI. As expected, the increase of calcium concentration impedes the precipitation of UO_3:$2H_2O$(cr) — schoepite. It was observed that the boundaries found by simulation corresponded pretty well to the experimental results. It can also be verified that the more charged species, i.e. $UO_2(CO_3)_3^{4-}$ and $CaUO_2(CO_3)_3^{2-}$, see their predominance domains increase with ionic strength.

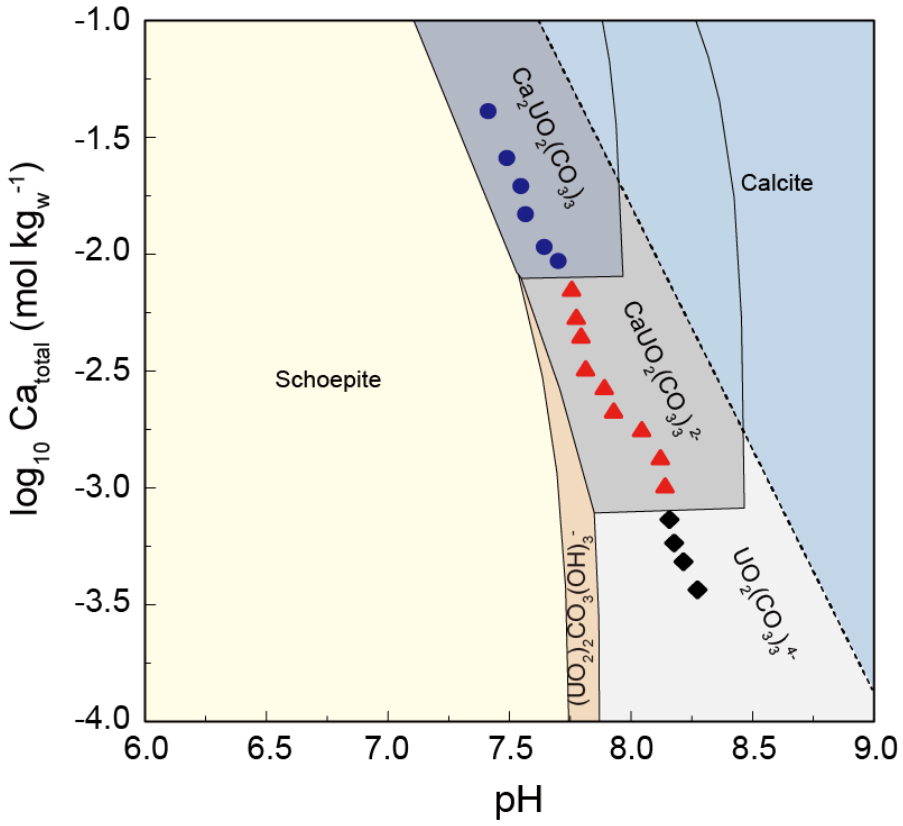


Figure 6. Predominance plots of Ca-UO_2-CO_3 system at [U(VI)] = 50 µmol kg_w^{-1}, P(CO_2) = $10^{-3.5}$ atm and I_m = 0.2 mol kg_w^{-1} NaCl. Experimental points giving slopes ca. 1 and 2 are highlighted with red triangles and blue filled circles, respectively. The black diamond represents the beginning of titration where the $UO_2(CO_3)_3^{4-}$ complex dominates.

3.3. Discussion on the values of ε and $\log_{10}\beta°$

the $\log_{10}\beta°$ values that we have determined are comparable to other determination in the literature, specific ion interaction coefficients determined in this work are different from literature data,[9,13] and different from other -2 bearing charge complexes — see Table S4 of the SI. It is often considered in literature that like-charged ions do share comparable ε values in analogy. This was specifically the case for $CaUO_2(CO_3)^{2-}$,[6,14] and also for other cases — see e.g. Table B-4 and B-5 in Guillaumont et al. [32]. After an analysis from tabulated data in Na^+ media, the highest found negative value is $\varepsilon(EdtaH_2^{2-},Na^+) = -(0.37 \pm 0.14)$ kg_w mol^{-1};[63] the highest positive value is $\varepsilon(Cu(OH)_4^{2-},Na^+) = (0.19 \pm 0.05)$ kg_w mol^{-1}.[64] Even it has no physical meaning, a grand average of the available data yields to $\varepsilon(X^{2-},Na^+) = -(0.09 \pm 0.12)$ kg_w mol^{-1}, illustrated by the repartition of the data in Figure S6 of the SI. Our value for $\varepsilon(CaUO_2(CO_3)_3^{2-},Na^+) = 0.29 \pm 0.11$ is higher than any other observed values — and markedly higher than $\varepsilon(UO_2(CO_3)_2^{2-},Na^+) = -(0.02 \pm 0.09)$ —; only $\varepsilon(Cu(OH)_4^{2-},Na^+)$ or $\varepsilon(UO_2F_4^{2-},Na^+)$ are contained in the standard deviation. Other multi-centred complexes as, e.g., UO_2Edta^{2-}, are showing negative values. This clearly shows that the analogy between like-charged ions is limited.

Ciavatta[65] proposed empirical relationships to estimate missing ε values of a product from the known ε values of the other reactants. In the case of $CaUO_2(CO_3)_3^{2-}$ one can postulate a 1:1 stoichiometry from eq. (2) and it comes

$$\varepsilon(CaUO_2(CO_3)_3^{2-},Na^+) = \frac{\varepsilon(UO_2(CO_3)_3^{4-},Na^+) + \varepsilon(Ca^{2+},Cl^-)}{2} \quad (14)$$

$$\varepsilon(CaUO_2(CO_3)_3^{2-},Na^+) = (0.07 \pm 0.06)\ kg_w\ mol^{-1}$$

that is showing a positive value, slightly higher, yet not significantly different from the grand average. It seems though that no other type of -2 charge bearing complex can be compared with $CaUO_2(CO_3)_3^{2-}$, and thus using other ε values in analogy seems not justified.

The case of $Ca_2UO_2(CO_3)_3(aq)$ is more challenging as there are only a few data on globally neutral species. Even if the common hypothesis of a nil value is used very often,[31,32] Ciavatta[65] proposed ε values for chloride, bromide, iodide, thiocyanate, and hydroxide complexes of Cd^{2+}, Hg^{2+}, and Pb^{2+} in perchlorate media; Zhang and Muhammed proposed a value for $Zn(OH)_2(aq)$ complex.[66] The grand average value of $\varepsilon(M(aq),NaClO_4) = -(0.01 \pm 0.06)$ kg_w mol^{-1} seems to confirm the common hypothesis of a nil value.

Nevertheless, other determinations of inorganic complexes do not follow this general trend. Ciavatta[65] determined $\varepsilon(Hg(OH)_2(aq),NaClO_4) = 0.2\ kg_w\ mol^{-1}$, and proposed that this positive value was linked to the formation of a hydrated oxocation complex $HgO(H_2O)_x$. Plyasunova, *et al.*[67] proposed $\varepsilon(Co(OH)_2(aq),NaClO_4) = -(0.15 \pm 0.10)\ kg_w\ mol^{-1}$. One can also note the $\Delta\varepsilon = (0.14 \pm 0.36)\ kg_w\ mol^{-1}$ $Cu(OH)_2(aq)$ in $NaClO_4$,[68] which would yield in $\varepsilon(Cu(OH)_2(aq), NaClO_4) = (0.18 \pm 0.36)\ kg_w\ mol^{-1}$ using ε from Guillaumont, *et al.*[69] and Ciavatta.[65] Powell, *et al.*[70] proposed $\Delta\varepsilon = -(0.05 \pm 0.03)\ kg_w\ mol^{-1}$ for the formation of $Zn(SO_4)(aq)$ in $LiClO_4$ media, which would yield in $\varepsilon(Zn(SO_4)(aq),LiClO_4) = (0.25 \pm 0.06)\ kg_w\ mol^{-1}$ using ε from Guillaumont, *et al.*[69] Otherwise, Ciavatta,[65] Hummel et al.,[63] and Fromentin and Reiller[42] proposed ε values for globally neutral organic species that range from the zwitterion ethylenediaminetetracetic acid, $\varepsilon(EdtaH_4(aq),NaClO_4) = -(0.29 \pm 0.14)\ kg_w\ mol^{-1}$, to the adipic acid, $\varepsilon(AdipateH_2(aq),NaCl) = (0.105 \pm 0.005)\ kg_w\ mol^{-1}$. It is also noteworthy that for adipic acid, the specific ion interaction coefficients proposed by Fromentin and Reiller[42] is significantly different in NaCl and $NaClO_4$ — the perchlorate case being close to the nil value hypothesis. From this analysis, it seems that the hypothesis of a nil value for the ε values of neutral species is not always justified.

Considering that $Ca_2UO_2(CO_3)_3(aq)$ is a 1:2 complex regarding eq. 2, and using the empirical relationship from Ciavatta[65] it comes,

$$\varepsilon(Ca_2UO_2(CO_3)_3(aq),NaCl) = \frac{\varepsilon(UO_2(CO_3)_3^{4-},Na^+) + 2\varepsilon(Ca^{2+},Cl^-)}{3} \qquad (15)$$

$$\varepsilon(Ca_2UO_2(CO_3)_3(aq),NaCl) = (0.09 \pm 0.04)\ kg_w\ mol^{-1}$$

which is positive, but is not giving a value as high as the one we are obtaining.

It can be inferred that for $Ca_2UO_2(CO_3)_3(aq)$ the common hypothesis of a nil value for ε does not seem to be justified either. It is noteworthy that Ciavatta[65] proposed another empirical relationship based on ionic radius, the values of which are not easy to retrieve for the $Ca_nUO_2(CO_3)_3^{(4-2n)-}$ complexes.

The implications of the different thermodynamic constants and specific interaction coefficients can be seen as a function of I_m through the variation of the activity coefficients (Figure 7a), and thermodynamic constants (Figure 7b). It is clearly shown that our results and extrapolations for $CaUO_2(CO_3)_3^{2-}$ are perfectly in agreement with the determinations in

$NaNO_3$,[12] NaCl,[14,15] and $NaClO_4$.[15] For $Ca_2UO_2(CO_3)_3(aq)$, there is a very good agreement with other obtained data,[8,12,15] when there is slight overestimation of Bernhard et al.,[5] and a slight underestimation of Endrizzi and Rao.[14] Up to 1 mol kg_w^{-1} one can notice that the values that we are proposing allows a very good representation of the $Ca_nUO_2(CO_3)_3^{(4-2n)-}$ complexes comportment. The comparison with the estimation of Kalmykov and Choppin[9] shows that our estimation is in agreement until I_m = 0.5 mol kg_w^{-1}, but do not allow understanding the comportment in more concentrated $NaClO_4$ medium, which would require further works accounting for the discussion in Guillaumont et al.,[32] and recent theoretical modeling.[33,71] The same comment applies to the evolution of $MgUO_2(CO_3)_3^{2-}$ proposed in Dong and Brooks,[13] as the influence of ionic strength seems very high and does not compare favourably with our results on $CaUO_2(CO_3)_3^{2-}$, which would be considered as an analogue component. Further works are clearly required to decipher these comportments, for instance in high ionic strength medium containing magnesium.[72,73]

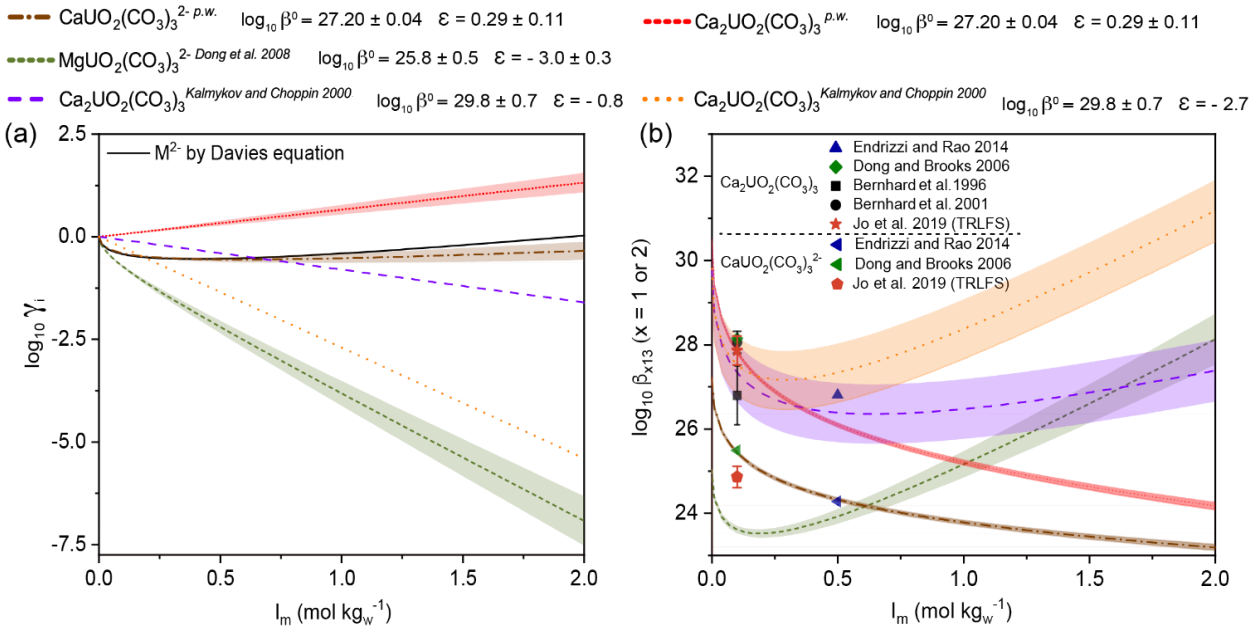


Figure 7. Variations of activity coefficients (a) and formation constants (b) for the $M_nUO_2(CO_3)_3^{(4-2n)-}$ complexes (M being Mg or Ca) as a function of molal ionic strength.

3.4. Structural implications for ternary species

The difference between these species, and other -2 charge bearing complexes, drew our attention to the molecular structures and actual electric charges of these species. Actually, complexation by alkali and alkaline earth metals is generally considered as weak ligand binding since the attraction between opposite-charged ions is marginally stronger than that

of simple electrostatic interaction.[74] A specific term is used in SIT to describe this (partial) association, and it should be noted that the extent to which cations form complexes varies widely in solution.[75] For $Ca_nUO_2(CO_3)_3^{(4-2n)-}$ species, the alkaline earth ions is locating in the second shell outside the inner shell for the three carbonates. Several EXAFS studies reported close bond distances for U-Ca shell, structurally exhibiting the manifold patterns of Ca-UO_2-CO_3 species.[7,8,16-18] Lee et al.,[7] and Kelly et al.,[16] respectively reported 4.15 and 4.1 Å for U-Ca in aqueous solution, which are in agreement with a previous study that proposed the value for R(U-Ca) = 4.05 Å in the corresponding solid — i.e. liebigite $Ca_2UO_2(CO_3)_3$(aq):$10H_2O$.[18] These results confirmed the similar structures existing in $Ca_2UO_2(CO_3)_3$(aq) complex independent of its state. However, the principal limitation of EXAFS is that the interpretation of data is often interfered by the very close distances of R(U-Ca) and R(U-O_{dist}).[7]

The role of cation in complexation has been investigated through theoretical modelling. The counter-ion effects of Ca^{2+} were proven to help stabilizing the fourfold negatively charged complex $UO_2(CO_3)_3^{4-}$ in aqueous environment with hybrid quantum mechanical/molecular mechanical molecular dynamics simulations.[76,77] Furthermore, classical molecular dynamics simulations have successfully described the impact of Na^+ on the binding between $UO_2(CO_3)_3^{4-}$ and Ca^{2+} ions by simulating the effect of 0.1 mol L^{-1} NaCl as background electrolyte.[71] The presence of sodium provoked a distortion of carbonate denticity and thus yielded space for entering one water molecule in the primary coordination sphere in $CaUO_2(CO_3)_3^{2-}$. As a consequence, an alteration in coordination number was induced in the equatorial plan of UO_2^{2+}, whereas in $Ca_2UO_2(CO_3)_3$(aq), sodium solely exacerbated the asymmetry of two calcium ions without changing the coordination number.

These findings provide indication for detectable influence of Na^+ on the structures of ternary species, which may give reasons for the positive and relatively large ε values in our study. Ion-pair formation most likely accounts for the strong dependence of ε on electrolyte concentration. The results of this study further indicate that the conventionally adopted value of $\varepsilon(UO_2(CO_3)_2^{2-},Na^+)$ to $\varepsilon(CaUO_2(CO_3)_3^{2-},Na^+)$ by analogy is questionnable. The affinity of Na^+ with globally neutral complex could yield a globally positively charged-complex, which has been proposed by theoretical calculations,[33] and maybe suggested by our experimental results. Besides, as suggested by previous investigators, the nil value of ε for like-charged ions should be treated carefully, because the ion-solvent interaction is underestimated according to the assumption of SIT.[78,79]

3.5. Practical applications

3.5.1. Practical application to the case of radioactive waste management

Once the determined thermodynamic constants of $Ca_nUO_2(CO_3)_3^{(4-2n)-}$ complexes allow predicting aqueous speciation accurately up to I_m = 1 mol kg_w^{-1} in NaCl-based medium, the first application is the calculation of the uranium speciation in a water composition representative of a clay host rock for a geological repository for radioactive wastes. Compositions of water in equilibrium with a clay rock, which can be the host rock of a radioactive waste repository, were proposed in the Belgian context of the Boom clay,[34] and in the French context of the Callovo-Oxfordian clay.[35] Using thermodynamic data from Guillaumont et al.,[32] if one considers that uranium is mostly under its +IV redox state under these conditions, the solid phase controlling the solubility is either UO_2(am,hyd) for the most soluble one, or UO_2(cr) for the most insoluble one. The very low solubility of these two phases, and the concentration of carbonate in these systems, prevents the formation of polynuclear species.

Up to now, the available data in the framework of the SIT[32] are not sufficiently complete to perform a calculation in a real situation. It would require the addition of thermodynamic data from other sources. Hence, we have used the Thermochimie 9b database — the sit.dat database file — provided with PhreeqC,[61,62] which contains the data from Guillaumont*, et al.*[32] for uranium, to perform the theoretical speciation calculation — the selection of data can be found on the web pages.[80] In this version of the database, $Ca_nUO_2(CO_3)_3^{(4-2n)-}$ complexes from Dong and Brooks[12] are present, with no ε values, which mean that the ε values are nil. The Mg^{2+}, Sr^{2+}, and Ba^{2+} complexes are not implemented.[7,10,12,13] We have made the choice to implement the Mg^{2+} and Sr^{2+} complexes from Dong and Brooks[12] as an estimation of their potential importance in the input PhreeqC file with no ε values.

The redox potentials — Eh_{SHE} = –274 mV, t = 16°C, pH 8.5 for the Mol reference water in de Craen*, et al.*[34], and Eh_{SHE} = –163 mV at pH 7.1 for solution A in Gaucher*, et al.*[35] — are fixed by a partial pressure of dioxygen calculated from the Eh_{SHE} and temperature of the water — $P(O_2) = 10^{-68.67}$ and $10^{-65.83}$ atm for de Craen*, et al.*[34] and Gaucher*, et al.*[35], respectively.

The solubility and aqueous speciation of uranium between pH 7 and 9 for the two water compositions are shown in Figure 8. The speciation results are markedly different because of the differences in total carbonate, calcium and magnesium concentrations, and Eh values. In the case of the Boom Clay water (Figure 8a,b),[34] even with a lower Eh value, the carbonate concentration in the Boom Clay water stabilizes the different triscarbonatouranyl complexes at the expenses of $U(OH)_4$(aq). The marked change in uranium speciation between $CaUO_2(CO_3)_3^{2-}$ and $UO_2(CO_3)_3^{4-}$ at pH 8.2 corresponds to the precipitation of dolomite ($CaMg(CO_3)_2$), which also affects the $MgUO_2(CO_3)_3^{2-}$ and $Ca_2UO_2(CO_3)_3$(aq) complexes. In the

case of the Callovo-Oxfordian water (Figure 8c,d),[35] the lower carbonate content but high calcium concentration yields to the predominance of $M_nUO_2(CO_3)_3^{(4-2n)-}$ complexes at pH values lower than 8.5, and to the predominance of $U(OH)_4(aq)$ at higher pH values. In both cases, the $MgUO_2(CO_3)_3^{2-}$ complex should be minor; the $SrUO_2(CO_3)_3^{2-}$ complex should be even minor.

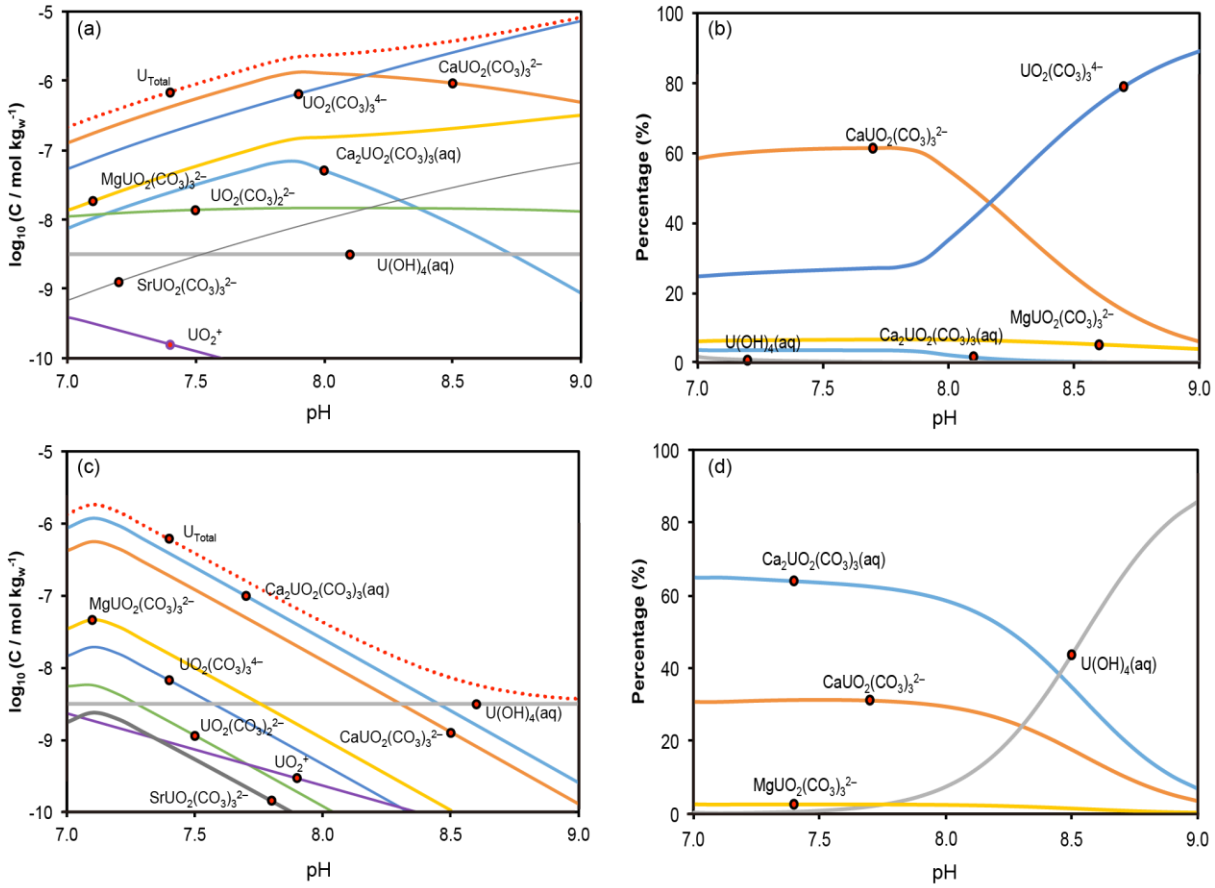


Figure 8. Solubility of UO_2(am,hyd) (a,c) and aqueous speciation of uranium (b,d) between pH 7 and 9 for Boom[34] (a,b) and Callovo-Oxfordian[35] (c,d) clay equilibrium waters using thermodynamic data from the Thermochime 9b database,[80] implementing $MgUO_2(CO_3)_3^{2-}$ and $SrUO_2(CO_3)_3^{2-}$,[12] correcting the $Ca_nUO_2(CO_3)_3^{(4-2n)-}$ data with thermodynamic constants values from Table 1, and implementing specific ion interaction coefficient from Table 3: $P(O_2) = 10^{-68.67}$ *(a,b) and* $10^{-65.83}$ *(c,d) atm.*

3.5.2. Practical application to the case of uranium speciation in seawater

Another application is the distribution of ternary species as well as the effects of solvent ions in seawater. Different compositions of seawater were proposed in the literature. Large

amounts of calcium and magnesium led to the predominance of $M_nUO_2(CO_3)_3^{(4-2n)-}$ complexes after theoretical speciation calculations.[7,14,17] Knowing the particular dependence observed for the $MgUO_2(CO_3)_3^{2-}$ complex as a function of $NaClO_4$ ionic strength,[13] and the lack of information on the corresponding comportment in NaCl, we will only focus our discussion on $Ca_nUO_2(CO_3)_3^{(4-2n)-}$ complexes in the following.

Authors proposed theoretical speciation calculations using either the data from Dong and Brooks[12] in an average Mediterranean seawater,[17] or their own determinations using simplified seawater compositions.[7,14] The predominance of either the neutral $Ca_2UO_2(CO_3)_3(aq)$ complex,[14,17] or the -2 charge bearing $CaUO_2(CO_3)_3^{2-}$ complex,[7] was obtained. However, the water composition is relatively unbalanced — electrical balance is $4.15\ 10^{-2}$ eq using PhreeqC — and the activity correction is not clearly specified, but guessed as done through a simplified Debye-Hückel approximation — which is not applicable in seawater — in the former case;[17] in the latter case,[7,14] the water composition — simplified from Millero, *et al.*[81] — is equilibrated and SIT with the nil hypothesis for the ε values, which seems not justified (vide ante), was used. It seems awkward to assess which complex dominates the uranium speciation in seawater.

Millero et al. proposed the composition of a standard seawater,[81] which can be used to perform a similar exercise, applying the thermodynamic constants (Table 1) and specific ion interaction coefficients (Table 3) determined in this work — the $UO_2CO_3F^-$ complex,[32] absent from Thermochimie 9b database, is implemented. We are proposing the theoretical speciation calculation in Figure 9, where $CaUO_2(CO_3)_3^{2-}$ is dominating the speciation at pH > 7, and $Ca_2UO_2(CO_3)_3(aq)$ is a significant secondary species — in this example, the partial pressure of $CO_2(g)$ is calculated from the total carbonate concentration in Millero et al.,[81] i.e. $10^{-3.24}$ atm. This speciation is reminiscent of the one proposed by Lee, *et al.*[7], but with a slightly less important proportion of the $Ca_2UO_2(CO_3)_3(aq)$ complex. It is noteworthy that dolomite ($CaMg(CO_3)_2$) and calcite ($CaCO_3$) are showing positive saturation indices at pH values above 7.6 and 7.8, respectively (Figure S7 of the SI). This means that the initial seawater composition is oversaturated with regards of these two phases. For this exercise, the precipitation of the carbonate phases of alkaline earth metals was not required.

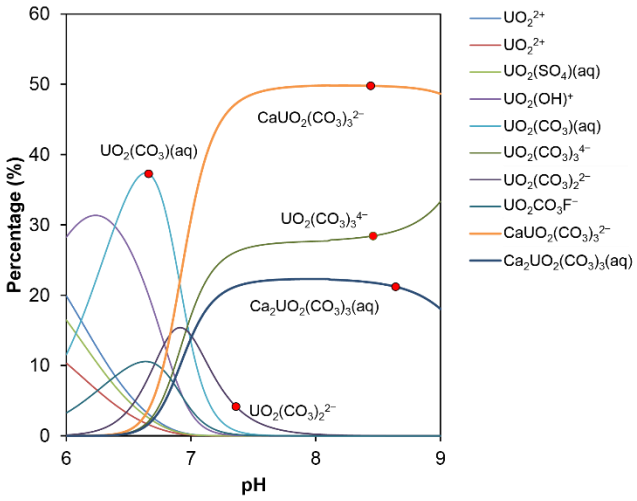


Figure 9. Theoretical speciation of uranium in a standard seawater composition,[81] P(CO_2) = $10^{-3.24}$ atm from the total carbonate concentration, and using the thermodynamic data from the Thermochimie 9b database,[80] correcting the $Ca_nUO_2(CO_3)_3^{(4-2n)-}$ data with thermodynamic constants values (Table 1) and implementing the specific ion interaction coefficients (Table 3) proposed in this work.

This exercise confirms the general predominance of $Ca_nUO_2(CO_3)_3^{(4-2n)-}$ in seawater and enlightens the need of comparable studies on the $Mg_nUO_2(CO_3)_3^{(4-2n)-}$ complexes at varying ionic strengths. As Mg/Ca concentration ratio is ca. 5 from Millero et al. seawater composition,[81] and $\beta^\circ(CaUO_2(CO_3)_3^{2-})/\beta^\circ(MgUO_2(CO_3)_3^{2-})$ is ca. 12 according to the estimation from Dong and Brooks,[12] $MgUO_2(CO_3)_3^{2-}$ should be significantly present in seawater — see the theoretical speciation proposed in Lee, *et al.*[7] Further works on the $Mg_nUO_2(CO_3)_3^{(4-2n)-}$ complexes vs. ionic strength are necessary to reduce the uncertainties on thermodynamic constants, and avoid the approximations for the specific ion interaction coefficients values.

4. Conclusion

The thermodynamic constants $\log_{10}\beta^\circ$ and Gibbs energies of formation $\Delta_f G^\circ_m$ of $CaUO_2(CO_3)_3^{2-}$ and $Ca_2UO_2(CO_3)_3(aq)$ have been extrapolated to infinite dilution from TRLS experiments in NaCl medium from I_m = 0.1 up to 1 mol kg_w^{-1}. The characteristics of the luminescence spectra are strikingly similar for all species, with gradually narrowed peak widths with complexation of calcium. The pH-dependent slope analysis was necessarily corrected with the Ringböm coefficient relative to $UO_2(CO_3)_3^{4-}$ complex according to the experimental methodology. As expected, no precipitation of schoepite or calcite was observed during the experiments. The stability constants are consistent with previously

reported data. Conversely, the values of the specific ion interaction coefficients $\varepsilon(CaUO_2(CO_3)_3^{2-},Na^+)$ and $\varepsilon(Ca_2UO_2(CO_3)_3(aq),NaCl)$ are strongly positive and markedly different from the previous estimation by analogy from like-charged ions, which may suggest a high affinity of Na^+ with $Ca_nUO_2(CO_3)_3^{(4-2n)-}$ species in solution. Similar studies at higher ionic strength and other background electrolyte such as sodium perchlorate media, and comparable studies on Mg^{2+} are highly desirable.

Acknowledgment

This work was financed by ONDRAF-NIRAS (contract DEN4857-CCHO 2018-0456/00/00). Dr. Hélène Isnard is acknowledged for her help during the dissolution of U_3O_8.

References

1. S. Cotton, *Lanthanide and Actinide Chemistry*, Wiley, Rutland, UK, 2006.
2. K. Maher, J. R. Bargar and G. E. Brown, Jr., *Inorg. Chem.*, 2013, **52**, 3510-3532.
3. J. I. Kim and B. Grambow, *Eng. Geol.*, 1999, **52**, 221-230.
4. M. Altmaier and T. Vercouter, in *Radionuclide Behaviour in the Natural Environment - Science, Implications and Lessons for the Nuclear Industry*, eds. C. Poinssot and H. Geckeis, Woodhead Publishing, Oxford, UK, 2012, DOI: 10.1533/9780857097194.1.44, ch. 3, pp. 44-69.
5. G. Bernhard, G. Geipel, V. Brendler and H. Nitsche, *Radiochim. Acta*, 1996, **74**, 87-91.
6. J. Y. Lee and J. I. Yun, *Dalton Trans.*, 2013, **42**, 9862-9869.
7. J.-Y. Lee, M. Vespa, X. Gaona, K. Dardenne, J. Rothe, T. Rabung, M. Altmaier and J.-I. Yun, *Radiochim. Acta*, 2017, **105**.
8. G. Bernhard, G. Geipel, T. Reich, V. Brendler, S. Amayri and H. Nitsche, *Radiochim. Acta*, 2001, **89**, 511-518.
9. S. N. Kalmykov and G. R. Choppin, *Radiochim. Acta*, 2000, **88**, 603-606.
10. G. Geipel, S. Amayri and G. Bernhard, *Spectrochim. Acta. A, Mol. Biomol. Spectrosc.*, 2008, **71**, 53-58.
11. C. Götz, G. Geipel and G. Bernhard, *J. Radioanal. Nucl. Chem.*, 2010, **287**, 961-969.
12. W. M. Dong and S. C. Brooks, *Environ. Sci. Technol.*, 2006, **40**, 4689-4695.
13. W. Dong and S. C. Brooks, *Environ. Sci. Technol.*, 2008, **42**, 1979-1983.
14. F. Endrizzi and L. F. Rao, *Chem.-Eur. J.*, 2014, **20**, 14499-14506.
15. Y. Jo, A. Kirishima, S. Kimuro, H.-K. Kim and J.-I. Yun, *Dalton Trans.*, 2019, **48**, 6942-6950.
16. S. D. Kelly, K. M. Kemner and S. C. Brooks, *Geochim. Cosmochim. Acta*, 2007, **71**, 821-834.
17. M. Maloubier, P. L. Solari, P. Moisy, M. Monfort, C. Den Auwer and C. Moulin, *Dalton Trans.*, 2015, **44**, 5417-5427.
18. S. Amayri, T. Reich, T. Arnold, G. Geipel and G. Bernhard, *J. Solid State Chem.*, 2005, **178**, 567-577.
19. M. Grivé, L. Duro, E. Colàs and E. Giffaut, *Appl. Geochem.*, 2015, **55**, 85-94.

20. M. H. Bradbury and B. Baeyens, *Applied Clay Science*, 2011, **52**, 27-33.

21. M. Marques Fernandes, N. Vér and B. Baeyens, *Appl. Geochem.*, 2015, **59**, 189-199.

22. W. M. Dong, W. P. Ball, C. X. Liu, Z. M. Wang, A. T. Stone, J. Bai and J. M. Zachara, *Environ. Sci. Technol.*, 2005, **39**, 7949-7955.

23. O. Prat, T. Vercouter, E. Ansoborlo, P. Fichet, P. Perret, P. Kurttio and L. Salonen, *Environ. Sci. Technol.*, 2009, **43**, 3941-3946.

24. C. Moulin, C. Beaucaire, P. Decambox and P. Mauchien, *Anal. Chim. Acta*, 1990, **238**, 291-296.

25. T. Vercouter, P. Vitorge, B. Amekraz and C. Moulin, *Inorg. Chem.*, 2008, **47**, 2180-2189.

26. C. Moulin, I. Laszak, V. Moulin and C. Tondre, *Appl. Spectrosc.*, 1998, **52**, 528-535.

27. C. Moulin, P. Decambox, V. Moulin and J. G. Decaillon, *Anal. Chem.*, 1995, **67**, 348-353.

28. G. Meinrath, *Radiochim. Acta*, 1997, **77**, 221-234.

29. Y. Kato, G. Meinrath, T. Kimura and Z. Yoshida, *Radiochim. Acta*, 1994, **64**, 107-111.

30. E. C. Jung, H. R. Cho, M. H. Baik, H. Kim and W. Cha, *Dalton Trans.*, 2015, **44**, 18831-18838.

31. I. Grenthe, L. Fuger, R. G. M. Konings, R. J. Lemire, A. B. Muller, C. Nguyen-Trung and H. Wanner, *Chemical Thermodynamics 1. Chemical Thermodynamics of Uranium*, North Holland Elsevier Science Publishers B. V., Amsterdam, The Netherlands, 1992.

32. R. Guillaumont, T. Fanghänel, V. Neck, J. Fuger, D. A. Palmer, I. Grenthe and M. H. Rand, *Update of the Chemical Thermodynamics of Uranium, Neptunium, Plutonium, Americium and Technetium*, OECD Nuclear Energy Agency, Data Bank, Issy-les-Moulineaux, France, 2003.

33. W. Wu, C. Priest, J. Zhou, C. Peng, H. Liu and D. E. Jiang, *J. Phys. Chem. B*, 2016, **120**, 7227-7233.

34. M. de Craen, L. Wang, M. Van Geet and H. Moors, *Geochemistry of Boom Clay pore water at the Mol site*, Report SCK•CEN-BLG-990, SCK•CEN, Mol, Belgium, 2004.

35. E. C. Gaucher, C. Tournassat, F. J. Pearson, P. Blanc, C. Crouzet, C. Lerouge and S. Altmann, *Geochim. Cosmochim. Acta*, 2009, **73**, 6470-6487.

36. I. Feldman, *Anal. Chem.*, 1956, **28**, 1859-1866.

37. G. G. Manov, N. J. Delollis and S. F. Acree, *J. Res. Nat. Bur. Stand.*, 1945, **34**, 115-127.

38. R. de Levie, *Adanced Excel for Scientific Data Analysis*, Oxford University Press, New York, 2005.

39. M. Moriyasu, Y. Yokoyama and S. Ikeda, *J. Inorg. Nucl. Chem.*, 1977, **39**, 2211-2214.

40. P. Moreau, S. Colette-Maatouk, P. Vitorge, P. Gareil and P. E. Reiller, *Inorg. Chim. Acta*, 2015, **432**, 81-88.

41. Y. Z. Kouhail, M. F. Benedetti and P. E. Reiller, *Environ. Sci. Technol.*, 2016, **50**, 3706-3716.

42. E. Fromentin and P. E. Reiller, *Inorg. Chim. Acta*, 2018, **482**, 588-596.

43. Y. Z. Kouhail, M. F. Benedetti and P. E. Reiller, *Chem. Geol.*, 2019, **522**, 175-185.

44. A. Ringböm, *Complexation in Analytical Chemistry: A Guide for the Critical Selection of Analytical Methods Based on Complexation Reactions*, Interscience Publishers, New York, NY, USA, 1963.

45. L. Maya, *Inorg. Chem.*, 1982, **21**, 2895-2898.

46. K. Muller, V. Brendler and H. Foerstendorf, *Inorg. Chem.*, 2008, **47**, 10127-10134.

47. I. Grenthe, D. Ferri, F. Salvatore and G. Riccio, *J. Chem. Soc., Dalton Trans.*, 1984, **0**, 2439-2443.

48. C. W. Davies, *Ion Association*, Butterworths, London, UK, 1962.

49. Y. Yokoyama, M. Moriyasu and S. Ikeda, *J. Inorg. Nucl. Chem.*, 1976, **38**, 1329-1333.

50. C. Ekberg and L. P. Brown, *Hydrolysis of Metal Ions*, Wiley-VCH, Weinheim, Germany, 2016.

51. V. Eliet, G. Bidoglio, N. Omenetto, L. Parma and I. Grenthe, *J. Chem. Soc., Faraday Trans.*, 1995, **91**, 2275-2285.

52. H. Anton and R. C. Busby, *Contemporary Linear Algebra*, Wiley & Sons, Inc., Pennsylvania, USA, 2002.

53. M. Moriyasu, Y. Yokoyama and S. Ikeda, *J. Inorg. Nucl. Chem.*, 1977, **39**, 2205-2209.

54. M. D. Marcantonatos, *J. Chem. Soc., Faraday Trans. I*, 1980, **76**, 1093-1115.

55. S. J. Formosinho, M. D. M. Miguel and H. D. Burrows, *J. Chem. Soc., Faraday Trans. I*, 1984, **80**, 1717-1733.

56. P. E. Reiller and J. Brevet, *Spectrochim. Acta, Part A*, 2010, **75**, 629-636.

57. B. Valeur, *Molecular Fluorescence: Principles and Applications*, Wiley-VCH, Weinheim, Germany, 2001.

58. D. J. Leggett, *Computational Methods for the Determination of Formation Constants*, Plenum Press, New York, USA, 1985.

59. D. G. Kinniburgh and D. M. Cooper, *Environ. Sci. Technol.*, 2004, **38**, 3641-3648.

60. D. C. Kinniburgh and D. M. Cooper, *PhreePlot: Creating Graphical output with PHREEQC*, http://www.phreeplot.org, 2011.

61. D. L. Parkhurst and C. A. J. Appelo, *User's Guide to PHREEQC (Version 2) — A Computer Program for Speciation, Batch-Reaction, One-Dimensional Transport, and Inverse Geochemical Calculations*, Report 99-4259, U.S. Geological Survey, Water-Resources Investigations, Lakewood, Colorado, USA, 1999.

62. D. L. Parkhurst and C. A. J. Appelo, *Description of Input and Examples for PHREEQC Version 3 — A Computer Program for Speciation, Batch-Reaction, One-Dimensional Transport, and Inverse Geochemical Calculations. Chapter 43 of Section A, Groundwater Book 6, Modeling Techniques*, U.S. Geological Survey, Denver, Colorado, USA, 2013.

63. W. Hummel, G. Anderegg, L. F. Rao, I. Puigdomènech and O. Tochiyama, *Chemical Thermodynamics 9. Chemical Thermodynamics of Compounds and Complexes of U, Np, Pu, Am, Tc, Se, Ni and Zr with Selected Organic Ligands*, North Holland Elsevier Science Publishers B. V., Amsterdam, The Netherlands, 2005.

64. N. V. Plyasunova, M. S. Wang, Y. Zhang and M. Muhammed, *Hydrometallurgy*, 1997, **45**, 37-51.

65. L. Ciavatta, *Ann. Chim. (Rome)*, 1990, **80**, 255-263.

66. Y. Zhang and M. Muhammed, *Hydrometallurgy*, 2001, **60**, 215-236.

67. N. V. Plyasunova, Y. Zhang and M. Muhammed, *Hydrometallurgy*, 1998, **48**, 153-169.

68. K. J. Powell, P. L. Brown, R. H. Byrne, T. Gajda, G. Hefter, S. Sjoberg and H. Wanner, *Pure Appl. Chem.*, 2007, **79**, 895-950.

69. R. Guillaumont, T. Fanghänel, J. Fuger, I. Grenthe, V. Neck, D. A. Palmer and M. Rand, *Chemical Thermodynamics 5. Update on the Chemical Thermodynamics of Uranium, Neptunium, Plutonium, Americium and Technetium*, North Holland Elsevier Science Publishers B. V., Amsterdam, The Netherlands, 2003.

70. K. J. Powell, P. L. Brown, R. H. Byrne, T. Gajda, G. Hefter, A.-K. Leuz, S. Sjöberg and H. Wanner, *Pure Appl. Chem.*, 2013, **85**, 2249-2311.

71. B. Li, J. Zhou, C. Priest and D. E. Jiang, *J. Phys. Chem. B*, 2017, **121**, 8171-8178.

72. J. F. Ranville, M. J. Hendry, T. N. Reszat, Q. L. Xie and B. D. Honeyman, *J. Contam. Hydrol.*, 2007, **91**, 233-246.

73. P. E. Reiller, L. Marang, D. Jouvin and M. F. Benedetti, in *The New Uranium Mining Boom. Challenge and Lessons Learned*, eds. B. Merkel and M. Schipek, Springer-Verlag, Berlin, Germany, 2012, DOI: 10.1007/978-3-642-22122-4_65, pp. 565-572.

74. J. N. Butler and D. R. Cogley, *Ionic Equilibrium: Solubility and pH Calculations*, Wiley & Sons, Inc., New York, USA, 1998.

75. Y. Marcus and G. Hefter, *Chem. Rev.*, 2006, **106**, 4585-4621.

76. A. O. Tirler and T. S. Hofer, *J. Phys. Chem. B*, 2014, **118**, 12938-12951.

77. A. O. Tirler and T. S. Hofer, *Dalton Trans.*, 2016, **45**, 4983-4988.

78. C. J. Downes, *J. Phys. Chem.*, 1970, **74**, 2153-2160.

79. M. H. Panckhurst and J. B. Macaskill, *J. Solution Chem.*, 1976, **5**, 469-482.

80. Thermochimie, http://www.thermochimie-tdb.com/).

81. F. J. Millero, R. Feistel, D. G. Wright and T. J. McDougall, *Deep-Sea Res. Pt. I*, 2008, **55**, 50-72.